Can mining wastewater be turned into a source of REE?

Separation of Rare Earth Elements in water with potentially disturbing elements

ivl
Swedish Environmental Research Institute

Report number: C11074
In cooperation with: Axolot Solutions Holding AB, KTH, RISE, Stockholm University
Author: Johan Strandberg, Sandra Fischer, Kåre Tjus, Fredrik Hedman, Therese Kärnman (IVL), Martin Ragnar (Axolot), Sritama Mukherjee, Ulrica Edlund (KTH), and Roshan Prabhakar, Latif Ullah, Niklas Hedin (SU)

Funded by: Mistra TerraClean

ISBN: 978-91-7883-779-3
Photo: Mikaela Bolternstern

[Rare Earth Elements; Critical Raw Materials; functionalized materials; separation technology]

Summary

This report presents the results from testing three separate process modules for the recovery of rare earth elements (REE) from dilute mine and industrial waters. The background to the work is the growing need to develop new, more efficient and environmentally benign methods than those currently available, as existing technologies often suffer from limitations in selectivity, cost-effectiveness and environmental performance. The evaluated modules – electrocoagulation, functionalized sorbents and HFSLM (hollow-fibre supported liquid membrane) – were assessed individually as potential components of a future integrated process chain for REE extraction. The work was carried out within the Mistra TerraClean research programme by IVL in collaboration with researchers from Stockholm University, RISE and KTH.

Pretreatment by electrocoagulation

Pilot-scale electrocoagulation using aluminium electrodes was tested on mine water from the Lovisa mine spiked with REE. The process showed selective removal of divalent transition metals (Zn^{2+}, Pb^{2+}, Cd^{2+}), while trivalent lanthanides remained in solution. This selectivity increased the REE/transition metal ratio by up to two orders of magnitude, potentially reducing the burden on subsequent process steps by lowering the concentration of interfering elements. Energy consumption was identified as a primary concern requiring optimisation, and the narrow pH window (4.8–5.2) demands careful control for successful implementation.

Development of functionalized sorbents

Six sorbent materials were synthesised and evaluated at bench scale for uptake of lanthanum (La^{3+}) from aqueous solutions. Aminopropyl-functionalised silica (SiAP) exhibited the highest adsorption capacity at 55 mg/g La^{3+}, while D2EHPA-impregnated silica (D2-SiAP) showed a three-fold increase in affinity despite lower overall capacity. Lignin-chitosan composites displayed broad pH tolerance but limited capacity (5 mg/g), and benzoxazine-based carbons showed moderate performance with good chemical stability. All sorbents were tested only in single-element solutions under controlled conditions. Regeneration protocols and breakthrough behaviour remain uncharacterised, and no scale-up to pilot columns has yet been conducted.

HFSLM Separation at Pilot Scale

HFSLM was tested using real mine water spiked with REE concentrations ranging from ng/L to µg/L. One month of continuous operation was achieved with over 90% efficiency, representing a significant improvement compared with previously published results. Through careful pH control, selective separation of individual rare earth elements was demonstrated in the tested matrices. The technique reduced solvent consumption by one to two orders of magnitude compared with conventional mixer–settler systems reported in the literature. pH control was found to be critical, including for maintaining membrane function, as pH levels above 3 led to gel formation, substantially reducing capacity. Losses of the extractant (D2EHPA in kerosene) were relatively small during operation, although some replenishment will be required upon scale-up. Reducing extractant losses will lower operating costs—given the high cost of the chemical—and decrease overall solvent use.

Integrated assessment

Overall, this research provides important insights into membrane-based recovery of rare earth elements (REE) from dilute streams and demonstrates that selective separation of individual REE is achievable through pH control. However, the technologies are still in a developmental phase. Realising their full potential will require addressing the operational and economic challenges identified here, particularly those related to long-term stability and cost-effectiveness. At the same time, the compact system design, reduced consumption of organic solvents and the demonstrated selectivity constitute strong incentives for continued development.

Conclusions

The research demonstrates the technical feasibility of individual process modules for REE recovery from dilute streams. Each module shows potential within specific operational windows—electrocoagulation for selective metal removal at controlled pH, sorbents for pre-concentration of REE and HFSLM for final separation and up-concentration. The modules, however, are positioned at different technology readiness levels (TRL): HFSLM is demonstrated at pilot scale (TRL 4–5), electrocoagulation partially at pilot scale (TRL 5–6) and the sorbents remain at bench scale (TRL 3–4).

Progress towards industrial implementation will require evaluating the technologies within an integrated process context, assessing their economic viability and demonstrating long-term operational performance. Priorities include scaling up the most promising sorbents to pilot columns, extending HFSLM testing to 3–6 months and subsequently testing all three modules in series based on the

actual water chemistry. The results constitute valuable proof-of-concept data but should be interpreted as highly promising early-stage research requiring substantial further development before industrial application is feasible.

Sammanfattning

Denna rapport presenterar resultaten från testning av tre separata processmoduler för återvinning av sällsynta jordartsmetaller (REE) från utspädda gruv- och industrivatten. Bakgrunden till arbetet är det växande behovet av att ta fram nya, mer effektiva och miljömässigt skonsammare metoder än de som används idag, eftersom befintliga tekniker ofta har begränsningar vad gäller selektivitet, kostnadseffektivitet och miljöpåverkan. Modulerna – elektrokoagulering, funktionaliserade sorbenter och HFSLM (hollow-fibre supported liquid membrane) – utvärderades var för sig som potentiella delar i en framtida integrerad processkedja för REE-utvinning. Arbetet utfördes av IVL Svenska Miljöinstitutet inom ramen för forskningsprogrammet Mistra TerraClean, i samarbete med forskare från Stockholms universitet, RISE och KTH.

Förbehandling med elektrokoagulering

Elektrokoagulering i pilotskala med aluminium-elektroder testades på gruvvatten från Lovisagruvan som spetsats med REE. Processen visade selektiv avskiljning av tvåvärda övergångsmetaller (Zn^{2+}, Pb^{2+}, Cd^{2+}), medan trivalenta lantanider behölls i lösning. Denna selektivitet ökade REE/övergångsmetallförhållandet med upp till två tiopotenser, vilket potentiellt kan minska belastningen på efterföljande processteg genom att minska mängden störande element. Dock identifierades energiförbrukning som ett primärt bekymmer som behöver optimeras, och det smala pH-intervallet (4,8–5,2) kräver noggrann kontroll för att implementeringen ska lyckas.

Utveckling av funktionaliserad sorbenter

Sex sorbentmaterial syntetiserades och utvärderades i bänkskala för upptag av lantan (La^{3+}) från vattenlösningar. Kisel funktionaliserad med aminopropyl (SiAP) visade högst adsorptionskapacitet med 55 mg/g La^{3+}, medan D2EHPA-impregnerad silika (D2-SiAP) uppvisade tredubblad affinitet trots lägre kapacitet. Lignin-chitosan-kompositer hade bred pH-tolerans men begränsad kapacitet på 5 mg/g, och bensoxazinbaserade kol visade måttliga resultat med god kemisk stabilitet. Alla sorbenter testades endast med enskilda elementlösningar under kontrollerade förhållanden. Regenereringsprotokoll och genombrottsbeteende är fortfarande okarakteriserade och uppskalning till pilotkolonner har inte genomförts.

HFSLM-separation i pilotskala

HFSLM testades med verkligt gruvvatten som spikades med REE-koncentrationer från ng/L till µg/L. En månads kontinuerlig drift uppnåddes med över 90 %

effektivitet, vilket är en betydande förbättring jämfört med tidigare publicerade resultat. Genom noggrann pH-kontroll kunde selektiv separation mellan enskilda sällsynta jordartsmetaller demonstreras i provmatriserna. Tekniken minskade behovet av lösningsmedel med en till två tiopotenser jämfört med konventionella mixer-settler-system enligt litteraturen. pH-kontroll visade sig vara avgörande, även för att upprätthålla membranens funktion, då pH-nivåer över 3 ledde till gelformation, vilket avsevärt minskade kapaciteten. Under driften var förlusterna av extraktionsmedlet (D2EHPA i fotogen) relativt små, men viss påfyllning kommer att krävas vid uppskalning. Att minska förlusterna av extraktionsmedel kommer sänka driftskostnaderna, där kemikalien är en stor del, och minska kemikalieanvändningen.

Sammantaget ger denna forskning viktiga insikter om membranbaserad återvinning av sällsynta jordartsmetaller (REE) från utspädda strömmar och visar att selektiv separation av enskilda REE är möjlig genom pH-styrning. Teknikerna befinner sig dock fortfarande i en utvecklingsfas. För att realisera deras potential krävs att de driftmässiga och ekonomiska utmaningar som identifierats här hanteras, särskilt kopplat till stabilitet över längre tidsperioder och kostnadseffektivitet. Samtidigt utgör den kompakta designen, den minskade användningen av lösningsmedel och den uppvisade selektiviteten starka incitament för fortsatt utveckling.

Slutsatser

Forskningen visar den tekniska genomförbarheten för enskilda processmoduler för REE-återvinning från utspädda strömmar. Varje modul visar potential inom specifika driftsfönster – EC för selektiv metallavskiljning vid kontrollerat pH, sorbenter för förkoncentrering av REE och HFSLM för slutlig separation och uppkoncentrering. Modulerna befinner sig dock på olika teknologimognadsnivåer (TRL), där HFSLM är i pilotskala (TRL 4-5), EC delvis demonstrerad i pilotskala (TRL 5-6) och sorbenter kvarstår i bänkskala (TRL 3-4).

Arbetet mot industriell implementering kommer innebära att teknikerna måste sättas i en processkontext, utvärderas ekonomiskt och driftas under längre tider. Prioriterat är att skala upp de mest lovande sorbenterna till pilotkolonner, förlänga HFSLM-tester till 3–6 månader och därefter testa alla tre moduler i serie baserat på den faktiska vattenkemin. Resultaten utgör värdefulla proof-of-concept-data men bör läsas som mycket lovande tidig forskning som kräver betydande vidareutveckling innan industriell tillämpning kan ske.

Table of contents

1 Introduction

This work was carried out between 2022 and 2025 and was funded by the Mistra TerraClean programme.

1.1 Background

Rare-earth elements (REEs) underpin many low-carbon and high-performance technologies, including permanent-magnet wind turbines, electric-vehicle motors, and photonic devices. Global demand is rising steadily, yet primary production is concentrated in a few regions, while conventional extraction routes generate extensive solvent inventories and acidic waste. Recovering REEs from dilute secondary streams—mine drainage, metallurgical process water or industrial effluents—could diversify supply and lower the overall environmental footprint, but such waters contain REEs only in the ng/L–µg/L range and are rich in competing ions. Achieving selective, cost-effective separation at these concentrations, therefore, remains a technical challenge.

1.2 Membrane-based alternatives to conventional extraction

Mixer–settler solvent extraction is the dominant industrial technology for primary REE separation. While highly selective when operated in multi-stage cascades, it is chemical- and energy-intensive and scales poorly to high-volume, low-grade feeds. Hollow-fibre supported liquid membranes (HFSLM) represent a compact alternative in which the extractant is immobilised in the pores of hydrophobic fibres, providing a high area-to-volume ratio and sharply reducing solvent inventory. Laboratory studies, using HFSLM, have demonstrated separation factors comparable to those of mixer–settlers, along with one to two orders of magnitude lower reagent consumption. (Batchu and Binnemans, 2018; Kim et al., 2016). However, the method encounters several practical challenges when scaled up: 1) shear-induced emulsification that removes the organic phase, 2) gel formation of acidic extractants at moderate pH or high metal concentrations, 3) gradual wetting of membrane pores resulting in extractant loss, 4) interaction of acidic extractants and rare earth elements at moderate pH or high metal loading forming a third phase, and loss of chemicals in the strip solution. Additionally, it is

necessary to integrate extractants or carriers that function across different pH ranges if both light and heavy lanthanides are to be recovered (Alemrajabi et al., 2022).

1.3 State of the art and remaining gaps

Most published HFSLM studies employ synthetic solutions containing > 100 mg/L REEs and few competing ions. Under these controlled conditions, distribution ratios above 100 and fluxes of 20–40 mmol/m²×h have been reported. Real mine or process waters, by contrast, carry millimolar levels of Ca^{2+}, Mg^{2+}, transition metals and dissolved organic carbon (DOC), which can complex REEs or occupy extractant sites. There are only a handful of low-level studies (e.g., Kim et al., 2016) and virtually no multi-week pilot data documenting extractant degradation, membrane wetting dynamics, or shear limits under realistic flow conditions. In parallel, adsorptive pre-concentration has shown promise for boosting REE levels upstream of membranes; however, cross-comparisons are scarce, and the longevity of this process under repeated regeneration remains uncertain.

1.3.1 Project objectives

The present project, which is a part of the Mistra TerraClean research programme, addresses these deficiencies through an integrated experimental campaign that:

1. Evaluates the use of electrocoagulation (EC) for pre-treatment of undesired substances, such as transition metals, from mine water.
2. Benchmark three families of functional sorbents—modified silicas, lignin-based composites, and polybenzoxazine-functionalised carbons—under harmonised isotherm and kinetic protocols.
3. Evaluates a pilot-scale HFSLM unit for continuous and semi-continuous extraction of REEs from low-concentration feeds, including actual mining wastewater.
4. Quantifies long-term membrane stability, extractant loss and regeneration efficiency, thereby generating design criteria for industrial implementation.

1.3.2 Scope of the report

The report is organised to follow the separation train from influent to product. Section 2 details materials, pilot configuration and analytical techniques. Section 3

merges results and discussion, beginning with the removal of interfering species, then comparing sorbent capacities and kinetics, and finally analysing membrane performance, selectivity and durability. The concluding section synthesises these findings into recommendations for a modular, field-ready platform that couples pre-treatment, adsorptive concentration and HFSLM extraction for sustainable REE recovery.

2 Methodology

This study adopts a systems-oriented experimental design to evaluate rare-earth-element (REE) recovery from low-concentration aqueous streams. Work was organised in three hypothetically sequential modules, as shown in Figure 2-1. First, transition-metal interferents were removed or suppressed ("pre-treatment"). Second, REEs were pre-concentrated on functionalised sorbents. Third, the enriched solution was processed in a pilot-scale hollow-fibre supported liquid-membrane (HFSLM) unit to achieve selective extraction and up-concentration. Experiments were conducted at laboratory scale and in semi-continuous pilot mode, using both synthetic feeds and mine water from Lovisagruvan. Detailed procedures for each module are given below, followed by the analytical protocols standard to all stages.

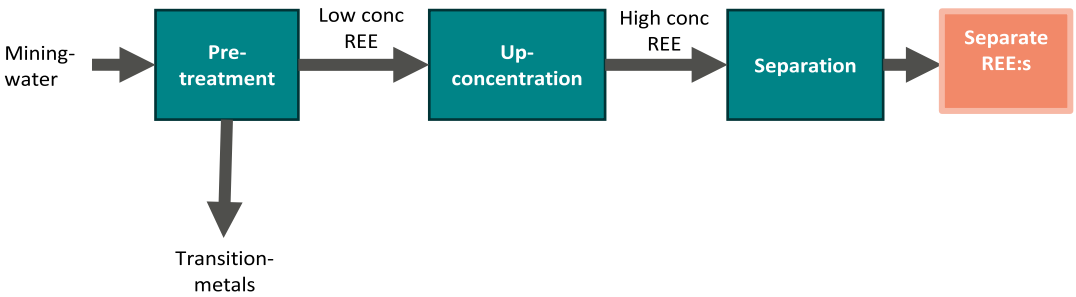

Figure 2-1. Hypothesised treatment train for the extraction of individual REEs from mining wastewater. Each step was tested separately in this project. The integration design will depend on the actual water composition in a future scale-up.

2.1 Pre-treatment of undesirable substances

Low-concentration mine waters typically contain millimolar levels of Fe, Mn, Zn, Pb and other divalent or trivalent metals that compete with REEs for sorption sites

and extractants. Selective removal of these matrix constituents improves subsequent recovery steps. Electrocoagulation (EC) was selected as the principal pre-treatment method due to its ability to generate in-situ $Al(OH)_3$ flocs through the anodic dissolution of aluminium. These flocs efficiently adsorb and co-precipitate a variety of transition metals, while, under controlled pH conditions, trivalent lanthanides remain in solution.

2.1.1 Electrocoagulation setup and protocol

Mine water from Lovisagruvan was spiked to 10 µg/L each of La^{3+}, Nd^{3+}, Dy^{3+} and Y^{3+} by IVL and handed over to Axolot Solutions Holding for testing using its continuous electrocoagulation technology AxoPur. The spiked water had a pH of 7.9 and was acidified to 4.8 just before testing by the addition of sulfuric acid. Tests were performed in bench-scale equipment at a flow rate of 50 L/h using aluminium electrodes. The tests were performed with a current density of 120 A/m², resulting in a tension of 30 V. A flocculation polymer was used to build up the flocs for separation following the EC treatment.

The water to be tested was stepwise alkalised using sodium hydroxide to elucidate the removal efficiency at seven different pH values. The pH naturally increases due to the EC treatment, resulting from the electrochemical reactions that occur. Table 2-1 shows the inlet and outlet pH values for each trial.

Table 2-1. pH conditions tested during seven electrocoagulation trials.

Trial	Inlet pH	Outlet pH
1	4.8	7.6
2	5.5	7.5
3	5.9	7.5
4	6.2	7.6
5	6.9	7.8
6	7.5	8.1
7	8.1	8.3

The clear phase of the treated waters was collected in acid-washed polyethylene vials (HNO_3, pH < 2) and sent to IVL for further analysis using ICP-OES for the four spiked REEs plus Zn, Pb, Cr, Fe, Ni, Cu, Co, As, Sr, Mo, Cd and Ba.

The EC experimental design thus enabled quantification of competing metal removal while tracking REE retention, establishing optimal pH windows for selective pre-concentration ahead of downstream sorption and membrane extraction processes.

2.1.2 Modified silica sorbents

The produced mesoporous silica was functionalised as follows.

a) Amine grafting: Calcined mesoporous silica was functionalised with amino silane by the wet grafting method. Silica was refluxed in toluene with amino silane ((3-Aminopropyl)triethoxysilane)(APTES) along with water. Water addition hydrates the adsorbent surface (increasing the hydroxyl groups) and leads to the polymerisation of the aminosilanes via siloxane bridges of free aminosilanes to other grafted aminosilanes. This functionalised sorbent is denoted as SiAP.

b) di(2-ethylhexyl)phosphoric acid (D2EHPA) impregnation: This organophosphorus extractant was loaded onto amine-grafted mesoporous silica (SiAP). The amount of D2EHPA was optimised as a function of representative REE (La) uptake. This sorbent is denoted as D2-SiAP.

c) Diglycolamide (DGA) functionalisation: This is a two-step modification process, in which the first step involves the synthesis of the DGA ligand using diglycolyl chloride and APTES (Juère et al., 2016). In the second step, the prepared mixture of modified silane was grafted onto the mesoporous silica. This functionalised sorbent is denoted as DG-SiAP.

Synthesised silica and functionalised sorbents were further characterised. The surface area and pore size distribution were analysed by N2 adsorption-desorption isotherms (Micromeritics ASAP 2020). The N2 isotherm plot and pore size distribution of pure mesoporous silica is shown in Figure 2-2a-b. The corresponding values for specific surface area (BET) and pore volume are 1007 m^2/g and 1.14 cm^3/g. The pore size ranges from 8 to 10 nm. The data on pore size distribution and pore volume indicate that the produced silica exhibits a mesoporous character.

Furthermore, the adsorption-desorption branch of the plot exhibits typical type IV isotherms with a well-pronounced capillary condensation step and a distinctive H1

hysteresis loop, characteristic of large cylindrical mesopores (Anyanwu et al., 2020). Morphological analysis of sorbents was done using scanning electron microscopy (SEM). SEM image of SBA-15 particles showing uniform, short rod-like morphology (Figure 2-2c)**.** The particles exhibit well-defined cylindrical shapes with an average length of 0.61 ± 0.18 μm, consistent with mesostructured silica synthesised under controlled conditions.

Thermogravimetric analysis (TGA) was used to determine the extent to which organic materials were successfully added (grafted) onto the surface of mesoporous silica. The percentage weight loss for pure silica, SiAP, D2-SiAP, and DG-SiAP was measured and found to be 4.35%, 14.37%, 16.32%, and 19.83%, respectively (see Figure 2-2d). The higher weight loss in modified samples compared to pure silica shows that the organic groups were successfully attached to the silica surface. For the D2EHPA-loaded sorbent and amine-grafted silica, the TGA results showed two distinct steps of weight loss, indicating a two-stage breakdown of the added organic materials. These findings also help to explain and support the results seen in the adsorption and uptake of lanthanum (La) by these materials.

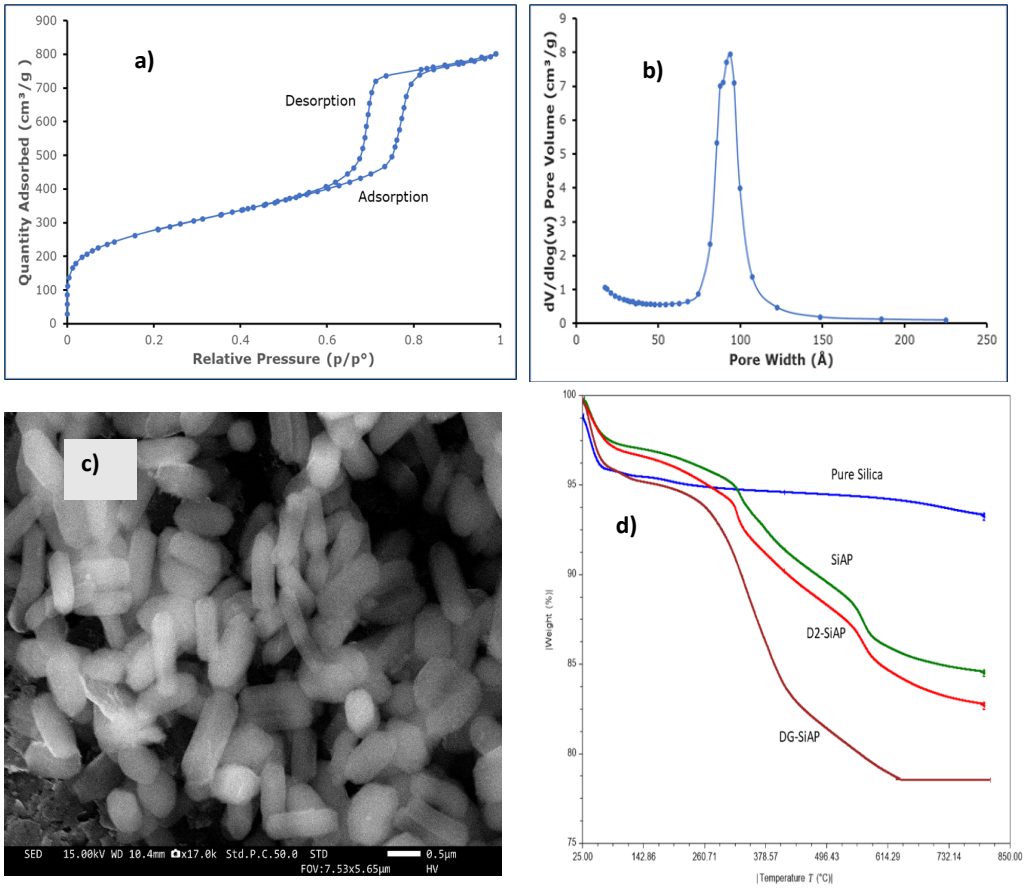

Figure 2-2. a) N_2 adsorption-desorption isotherms measured at -196 °C for the raw mesoporous silica; b) Pore size distribution (PSD) plot of raw mesoporous silica; c) Representative SEM image of pure mesoporous silica; d) Thermogravimetric analysis (TGA) curves of silica and functionalised sorbents

2.1.3 Functionalised lignin sorbents

The lignin-based material (ZLC) was synthesised via a one-pot aqueous reaction combining chitosan and a functionalised lignin, the latter prepared by the immobilisation of zwitterionic groups to kraft lignin. The resulting zwitterionic biocomposite features multiple charged functional groups (amine and carboxyl) for ion exchange and complexation. Chitosan served as a stabiliser, improving granule morphology and resistance to mechanical degradation during agitation or filtration. Such composites are desirable due to their renewable origin and tunable functionality.

The material demonstrated thermal and pH stability over a broad range and was tested under multiple pre-treatment and sorption scenarios. It is currently under patent review for potential application in mine water treatment systems (internal communication, IVL).

2.1.4 Carbon-based sorbents

Porous carbons serve as substrates that form an interpenetrating network consisting of an electron-conducting phase (carbon) and a fluid phase (polluted water). Incorporating functional groups at the interface between two phases—specifically on the surface of porous carbon—can yield advanced materials. These functional groups are capable of selectively binding to target metal ions, and their binding affinity can be adjusted electrochemically. Alternatively, the electrochemical characteristics of the functionalised porous carbon may change upon interaction with metal ions, effectively describing the behaviour of a sensor material.

In the new method to functionalise porous carbons, the porous carbons are partially impregnated with benzoxazine monomers. Synthesis and polymerisation of benzoxazines are illustrated in Figure 2-3. The monomers are allowed to spread within the porous structure, and any solvent, if used, is removed by evaporation under vacuum. Upon heating, the benzoxazines polymerise to form an immobilised polybenzoxazine network at the surface of porous carbon particles, termed PBz@Carbon, as illustrated in Figure 2-4.

Polybenzoxazine networks exhibit thermal and chemical stability, maintaining their structure under extreme pH conditions, elevated temperatures, and exposure to various solvents. This stability is attributed to the structure of the polymer backbone, which primarily consists of phenols linked by Mannich bridges. Cyclic oligomeric benzoxazine can be described as an aza calixarene, a type of structure recognised for its ability to bind metal ions (Chirachanchai et al., 2011).

The polybenzoxazine backbone contains segments similar to those of aza calixarenes, as shown in Figure 2-5, which demonstrate metal-binding capabilities. This structure enables polybenzoxazines to bind copper ions (Laobuthee et al., 2003) and also makes them suitable for regenerable mercury ion absorbents (Taskin et al., 2014). In polymers, aza calixarene-like motifs appear as helical arrangements within the backbone (Goward et al., 2003). PBz@Carbon consists of aza-calixarene analogues anchored to porous carbon surfaces. Furthermore, the absorbent properties of the metal ions are enhanced by the large surface area of the partially impregnated carbon particles. Until this project, PBz@Carbons have not been investigated for the absorption of rare earth metal ions.

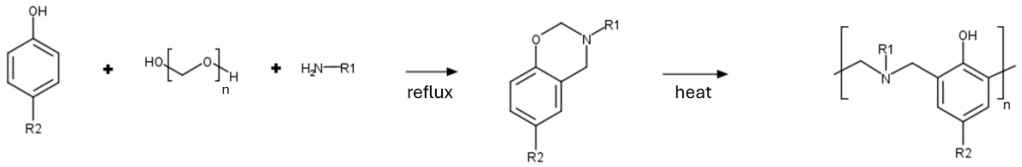

Figure 2-3. General schemes of synthesis and polymerisation of benzoxazines.

Figure 2-4. Impregnating porous carbons with benzoxazine monomer solutions, followed by drying, degassing, and heating, produced polybenzoxazine at the surface of carbon (PBz@Carbon).

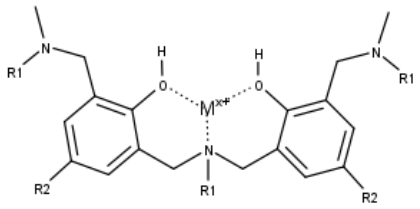

Figure 2-5. A dimer unit in polybenzoxazine coordinating a metal ion.

Hydrochar is a low-cost, sustainable adsorbent produced from wet biomass through hydrothermal carbonisation (HTC; Figure 2-6), a process that avoids the energy-intensive pre-drying step of traditional methods (Petsagkourakis et al., 2024). Besides its affordability and ease of preparation, its primary advantage lies in the abundance of oxygen-containing functional groups, such as carboxyl (−COOH) and hydroxyl (−OH), which are preserved during the HTC process. These groups offer numerous active sites for effectively binding metal ions through chelation and ion exchange, rendering hydrochar a highly efficient and environmentally friendly material for wastewater treatment.

To enhance the selectivity of hydrochar adsorbents for the selective removal of rare earth elements (REEs), further functionalisation can be achieved with relative ease. Functional groups such as amine (−NH_2), carboxyl (−COOH), and amide (−$CONH_2$) exhibit particular efficacy in adsorbing REEs, and in certain instances, they do so selectively (Li et al., 2025; Wilfong et al., 2020). Here, hydrochar adsorbents were synthesised with these functionalities in mind during the preparation process, incorporating precursors that render (-H_2) and (-COOH) groups. This targeted strategy led to the creation of additional active sites, thereby enhancing the

material's adsorption capacity. Two distinct materials, AAC-1 and AAC-2, were synthesised with varying functional material loadings to examine the impact of surface chemistry on adsorption performance. Morphologically, both materials exhibited a similar spherical appearance, as depicted in the SEM image (Figure 2-7).

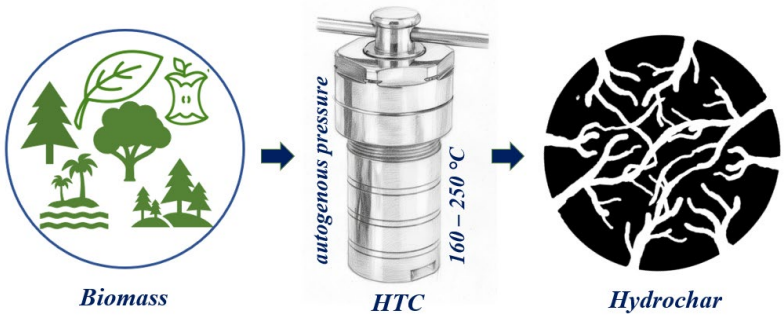

Figure 2-6. Simplified scheme for preparation of hydrochar adsorbent.

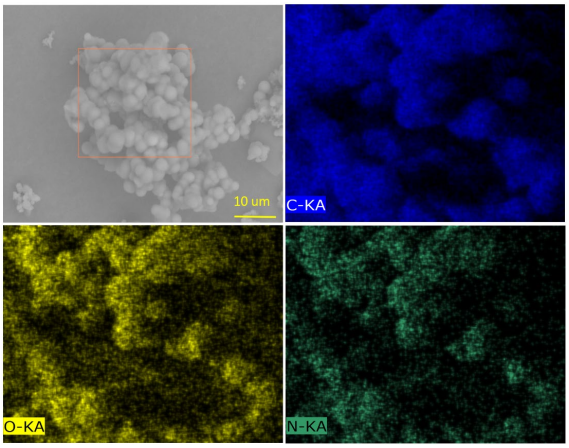

Figure 2-7. SEM and EDX analysis of hydrochar adsorbent material.

2.1.5 Sorption experiments

Adsorption experiments were conducted by considering key affecting parameters, such as time, dose, and pH, in batch mode. For analysis of the La concentration remaining in solution after adsorption, an aliquot of the solution was collected and filtered through a 0.45 µm syringe filter to separate the sorbent. The equilibrium concentration of La in the filtered solution was quantified using an in-house method, which employed the Arsenazo III dye and UV-Vis spectrophotometry (as described under 2.3 Analytical methods). The methodological detection limit (MDL) was found to be 0.018 ppm. The performance of the sorbents was assessed

by evaluating two parameters: uptake capacity (Q_e) and removal percentage (R), using the following Equation 2-1 and Equation 2-2 (Zhang et al., 2020):

$$Q_e = \frac{(C_0 - C_e)V}{m} \qquad \textit{Equation 2-1}$$

$$R(\%) = \frac{(C_0 - C_e)100}{C_0} \qquad \textit{Equation 2-2}$$

where C_o and C_e represent the Initial concentration and equilibrium concentration, respectively. Preliminary sorption tests were conducted to identify the optimal functionalisation conditions for each sorbent. For the amine-grafted sorbent, the APTES-to-silica weight ratio was varied as 5:1, 2:1, 1:1, 0.5:1, and 0.25:1. A noticeable decrease in La uptake (1 ppm) was observed only at the lowest ratio of 0.25:1 (APTES:Si). For all higher ratios, the uptake remained consistent at approximately 4.9 mg/g. Therefore, to ensure cost-effectiveness while maintaining performance, a ratio of 0.5:1 (APTES:Si) was selected for further studies. In the case of D2EHPA loading, it was observed that higher loadings rendered the silica surface increasingly hydrophobic, negatively affecting La adsorption. At a loading of 1.5 mmol/g, the La removal efficiency was 84.34%.

In contrast, at a lower loading of 0.19 mmol/g, the removal efficiency increased significantly to 98.74%. Based on this, a lower D2EHPA loading was chosen. The actual amount of D2EHPA loaded can be verified by the TGA curve presented above (Figure 2-2d), which shows a 1.80% weight loss compared to SiAP, confirming successful grafting. With the optimised functionalisation, comprehensive batch sorption tests were executed.

The effect of contact time was evaluated using a 1 ppm La concentration and a 5 mg sorbent dose. Irrespective of functionalisation, with an increase in time, the La removal efficiency and uptake increased. There was a rapid removal, within 15 minutes, of 61-78% of La, which had been adsorbed onto the surface. The uptake ranged from 3.07 to 4.97 mg/g. Diglycolamide-functionalised silica outperformed in terms of rapid uptake of La. No notable change in removal efficiency was observed beyond a contact time of 60 minutes, as the adsorption sites were utilised entirely. A higher La concentration (5 ppm) was also tested to study the effect of contact time, as equilibrium may not be achieved within 60 minutes during isotherm experiments involving a range of concentrations. At 5 ppm, the optimum contact time was found to be 180 minutes for all sorbents, except for DG-SiAP, which

required nearly 18 hours to reach equilibrium. Similarly, for ZLC and AC sorbents, the optimum times were 60 and 360 minutes, respectively.

To evaluate the effect of adsorbent dosage, experiments were conducted by varying the dose from 0.04 to 0.4 g/L, with a fixed contact time of 60 minutes. For SiAP and D2-SiAP, the optimum dose was found to be 0.2 g/L, while for DG-SiAP, it was 0.1 g/L. As the sorbent dose increased, a decrease in uptake capacity (Q_e) was observed, which is expected due to the aggregation of particles or the overlapping of active sites. It is speculated that higher adsorbent doses provide a greater number of active sites, leading to increased overall La removal, but lower uptake per unit mass of sorbent.

pH plays a crucial role in controlling both the speciation of La^{3+} ions and the surface charge of the adsorbent, thereby influencing the adsorption process. Using the previously optimised adsorbent dose and contact time, the pH of a 1 ppm La solution was varied from 2.0 to 7.4. As shown in Figure 2-8, both La removal and uptake were lowest under acidic conditions. This reduction in performance at low pH is likely due to protonation of the amine groups, which inhibits La^{3+} binding. Zeta potential analysis of SiAP supports this observation, showing a continuous decrease in surface charge with increasing pH and indicating an isoelectric point (IEP) at approximately pH 6 (Yadoun et al., 2024).

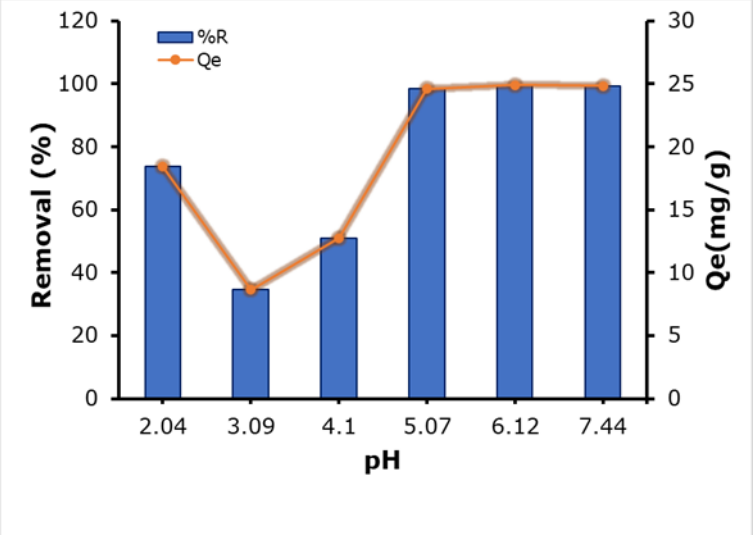

Figure 2-8. Effect of pH on La adsorption using SiAP sorbent.

2.1.6 Isotherm studies

Isotherm modelling can effectively assist in designing adsorption-based treatment systems. It can also help illustrate the mechanism and applicability of the adsorption process. Langmuir and Freundlich are the two well-known and applicable isotherm models for a single solute system. The Langmuir isotherm model assumes that the adsorbent surface contains active sites of uniform energy, which facilitates the monolayer adsorption process (Kalam et al., 2021). Once the active sites are occupied, the adsorbing molecules cannot interact with neighbouring molecules. Unlike the Langmuir isotherm, this empirical model can be applied to multilayer adsorption on heterogeneous sites. It assumes that the distribution of adsorption heat and the affinities toward the heterogeneous surface are nonuniform. In this work, we fitted the experimental data to the nonlinear forms of these isotherms (Equation 2-3 and Equation 2-4) to avoid the bias introduced by linearisation (Velazquez-Jimenez et al., 2018).

$$Q_e = \frac{Q_m K_L C_e}{1 + K_L C_e} \qquad \textit{Equation 2-3}$$

$$Q_e = K_f C_e^{l/n} \qquad \textit{Equation 2-4}$$

Where Q_e and C_e have the usual definitions as described earlier. Q_m (mg/g) represents the Langmuir maximum uptake or adsorption capacity, and K_L is the Langmuir adsorption constant, which is often interpreted as a measure of the binding strength. K_f and n correspond to Freundlich constants, and are related to adsorption capacity and adsorption intensity, respectively. Furthermore, the fitness of these models was evaluated not only as a function of R^2 but also considering error functions like chi-square ($\chi 2$), which is represented by Equation 2-5.

$$\chi^2 = \sum_{i=1}^{n} \frac{\left(q_{ecalc} - q_{eexp}\right)^2}{q_{eexp}} \qquad \textit{Equation 2-5}$$

2.2 Separation and up-concentration using hollow-fibre supported liquid membranes

Hollow-fibre supported liquid membranes (HFSLM) were employed to extract and concentrate rare earth elements (REEs) from low-concentration aqueous streams. The methodological focus was on (i) configuring a pilot unit that can be run in continuous or semi-batch modes, (ii) establishing a robust cleaning–conditioning–impregnation protocol, (iii) defining operating envelopes for pH, flow and pressure, and (iv) monitoring extractant loss and membrane stability over extended operation.

The separation principle of the HFSLM is outlined in Figure 2-9. Specifically, metal ions in the feed solution (left side in Figure 2-9) react at the feed-membrane interphase, forming complexes with an organic extractant that then diffuse through the membrane and deliver metal ions into the stripping solution (right side in Figure 2-9) at the membrane-strip solution interphase. The primary driving force behind metal transport is the difference in pH between the feed and strip solutions.

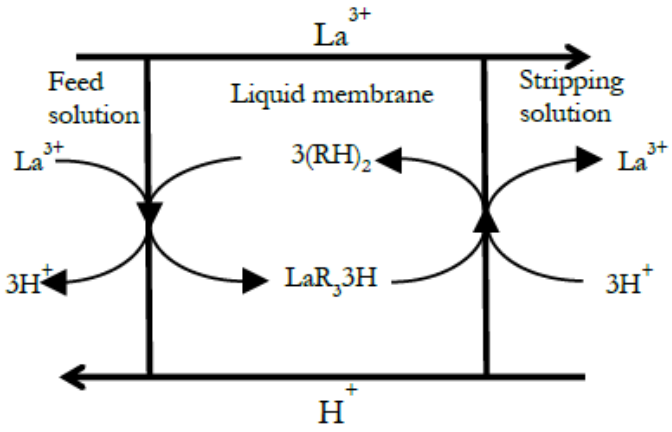

Figure 2-9. Separation principle of ions of lanthanides, here exemplified with Lanthanum (La3+) in supported liquid membrane extraction, where R represents an organic carrier. (Martinez, J et al 2018).

The main reactions can be described, for the trivalent lanthanides, as exemplified in Equation 2-6 for La.

$$La^{3+} + 3(HA)_2 \leftrightarrow LaA_3(HA)_3 + 3H^+ \qquad \textit{Equation 2-6}$$

Where A stands for the extractant without hydrogen, the liquid membrane consists of an organic extractant (or carrier) dissolved in an organic diluent. Common extractants are di-(2-ethylhexyl) phosphoric acid (D2EHPA) or (PC88A), and diluents are usually kerosene or isopar-L (Batchu and Binnemans, 2018).

2.2.1 Pilot configuration and hydraulic modes

The membrane module (Figure 2-10) consisted of hydrophobic polypropylene hollow fibres (0.1 μm nominal pore size, 8 m² effective surface area) mounted vertically in a stainless-steel housing. Two hydraulic schemes were used. In circulation mode, separately 10 to 1000 L feed and 2-10 L strip are recirculated continuously through the shell side and the lumen side of the hollow fibres, respectively. In semi-circulation mode, the feed solution was shuttled between two 100 L tanks across the membrane, creating discrete "passes" while the strip loop remained closed. For long-term testing, a 1000 L feed reservoir replaced the 100 L vessels. Nominal flow ranges were 50–180 L/h on the feed side and 75–185 L/h on the strip side, yielding residence times of 26-94 s for the feed in the fibre shell side, with a volume of 1.3 L, and 12-29 s for the strip in the fibre lumen, with a volume of 0.6 L.

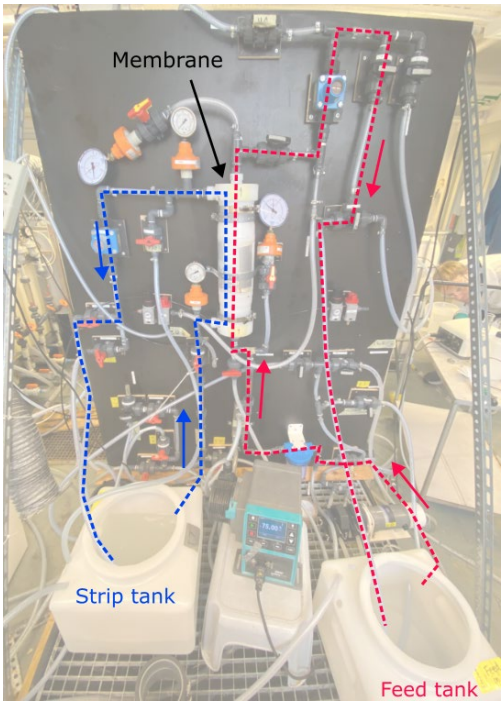

Figure 2-10. Set up of the pilot on hollow fibre-supported liquid membrane (HFSLM) for separation of REEs. The white cylinder in the centre is the membrane unit, and the strip (blue) and feed (red) solutions are assembled here in a circulating mode.

Feed solutions were prepared from either deionised, tap water or mine water, spiked with La, Nd, Y, and Dy at concentrations ranging from 25 to 170 mg/L. Zn (≈ 17 mg/L) was introduced in selected competitive-transport trials. The feed pH was adjusted to predetermined values (1.0, 1.5, 2.0, or 3.0) with hydrochloric acid in the feed tank. Strip solutions comprised 1-3 mol/L nitric or 0.5-4.5 M hydrochloric acid, conditions known to favour stripping of trivalent lanthanides (Batchu and Binnemans, 2018; Kim et al., 2016).

2.2.2 Cleaning, drying and impregnation protocol

Before each campaign, the module was flushed for 15 minutes with deionised water, followed by a 1% NaOH rinse (pH ≈ 10) for 30 minutes and a 0.1 mol/L HCl rinse (pH ≈ 1.5) for 15 minutes. Ethanol (96%, 5 L) was then circulated to displace residual water and any kerosene-containing extractant from earlier runs. The unit was dried for 24 hours with filtered air heated to 27-28 °C (relative humidity < 10%). Hydrophobic integrity was verified by pressurising the shell-side with deionised water at 4 bar; the absence of breakthrough confirmed that pores remained non-wetted.

For impregnation, a solution of 10 vol% di(2-ethylhexyl)phosphoric acid (D2EHPA) in kerosene was circulated through the lumen side under a differential pressure of 0.2 bar for 30 min. Approximately 300 mL of organic phase was retained in the fibre matrix; the remainder was recovered and weighed. This extractant–diluent formulation was selected based on its high distribution coefficients for light and middle REEs and its extensive use in HFSLM literature (Alemrajabi et al., 2022; Binnemans et al., 2013).

2.2.3 Operating protocols and variable-matrix trials

Routine experiments were conducted at ambient temperature (20 ± 1 °C). Feed pH was controlled within ±0.05 units. Flow rates were set using variable-speed peristaltic pumps (Masterflex L/S) that were calibrated weekly.

Stirring tests were conducted in a 10 L strip tank to assess the impact of droplet dispersion on mass transfer. A four-blade PTFE impeller (Ø 55 mm) at 300 rpm and, alternatively, a 40 mm PTFE-coated magnetic bar at 700 rpm were compared. In a follow-up trial, the strip vessel was replaced by a square (30 × 30 cm) tank to assess geometric effects on phase separation. Only the mechanical parameters are reported here; performance outcomes are presented in Section 3.3.

2.2.4 Instrumentation and online monitoring

Digital pressure sensors located upstream and downstream of the module recorded back pressure. Acid back diffusion was followed by measuring shifts in the pH. Total organic carbon (TOC) and total phosphorus (TP) were measured in both circuits to quantify the extractant loss by ICP analysis of REE and other metals. Arsenazo III was used to quantify yttrium during long-term tests. Arsenazo III dye was used in a long-term test with yttrium.

Samples (50 mL) of feed and strip solutions were taken every second pass in semi-circulation mode, or every 6 h in continuous circulation, filtered (0.45 µm), acidified to pH < 2, and stored at 4 °C pending ICP-OES analysis (Section 2.4).

2.2.5 Long-term operation and regeneration strategy

A sixteen-day continuous run was conducted, during which the HCl concentration for the strip solution was varied between 0.5 M and 4.5 M. Performance was monitored as above, using zinc as the model substance. On days 7 and 11, the strip acid was adjusted to evaluate the pH-driving force. The membrane was prepared before the start of a new cycle.

Before a second continuous, long-term test, a new membrane was prepared and tested for integrity. During continuous operation, different feedwaters were used, including pH-adjusted tap water and pH-adjusted tap water spiked with yttrium, as well as mining water.

For the first four days, pH-adjusted tap water was used in circulation mode to ensure the membrane remained intact, using the feed pH as an indicator. While in continuous operation, the feedwater was then switched, along with the operation mode, to run batch tests with controlled levels of yttrium spiked into tap water and mining water. After batch tests, the operation mode was switched back to circulation mode, and tap water was used again. A long-term test was conducted, using 5 mg/L yttrium in circulation mode with a 1000-litre feed tank.

A sixteen-day continuous run was conducted, during which the HCl concentration for the strip solution was varied between 0.5 M and 4.5 M. Performance was monitored as above, using zinc as the model substance. On days 7 and 11, the strip acid was replaced to evaluate different conditions. On day 9, the feed pH was stepped from 2.0 to 1.5 to probe transport-rate sensitivity. At the end of the run, the

module underwent a complete cleaning and impregnation protocol before the start of a new cycle. Regeneration efficiency was judged by restoring initial hydrogen back-diffusion rates and TOC baselines.

2.2.6 Equilibrium modelling for transport predictions

Membrane-transport data were interpreted with a mass-balance and equilibrium model adapted from Ni'am et al. (2020). Distribution ratios for La^{3+}, Nd^{3+}, Y^{3+} and Dy^{3+} between D2EHPA/kerosene and 1 mol/L nitrate media (Equation 2-6) were coded into an Excel simulation tool routine that simulated successive equilibrium stages inside the fibres. Feed-side speciation constants were taken from (Batchu and Binnemans, 2018). Stripping kinetics were assumed to be controlled by interfacial area and strip acid concentration; a rate constant was obtained by fitting early-time zinc data (Section 3.3). The model was used solely to plan operating envelopes; numerical predictions are not considered results and are therefore not reported in Section 3.

2.3 Analytical methods

A combination of spectrophotometric, elemental, and structural characterisation techniques was applied to assess sorption performance, material properties, and process behaviour across all experimental systems. Analytical protocols were harmonised to ensure comparability between different sorbents and treatment methods and were selected based on their relevance to trace element quantification and material stability.

Elemental analysis of rare earth elements (REEs) in aqueous samples was primarily conducted using inductively coupled plasma optical emission spectroscopy (ICP-OES). These analyses were performed at IVL's accredited laboratory using a Thermo Scientific iCAP 7000 series instrument. Calibration standards for La, Nd, Y, Dy, and Zn were prepared in the range of 1–200 µg/L, achieving detection limits of below 0.5 µg/L. Internal standards and quality controls were included in each analytical batch. To assess potential matrix effects, spike-and-recovery experiments were conducted in both synthetic mine water and tap water, following protocols similar to those described by Batchu and Binnemans (2018).

Arsenazo III is a metallochromogenic dye that forms stable chelate complexes with metal ions, depending on factors such as pH, metal concentration, and the presence of other cations or anions. One of its main advantages is its ability to form highly stable complexes in strongly acidic media, allowing for the spectrophotometric determination of lanthanum even in the presence of potentially interfering anions, such as phosphates, sulfates, and fluorides. However, Arsenazo III can also form complexes with divalent ions, such as calcium (Ca^{2+}), especially at higher pH values (Hogendoorn et al., 2018). Since lanthanides hydrolyse readily at low pH, the method benefits from acidic conditions that improve selectivity. To reduce interference from competing metal ions, like Ca^{2+}, the pH was optimised and kept below 3.0. Literature suggests that Arsenazo III forms 1:1 metal-dye complexes, with only one arseno group involved in metal binding (Basargin et al., 2000). Consequently, the La:dye ratio was carefully optimised during calibration. When the La: dye molar ratio exceeds 1, the linearity of absorbance is lost, which is also visually evident as a colour change from pink at lower La concentrations (e.g., 15 ppb) to violet at higher concentrations (e.g., 750 ppb; Figure 2--). Absorbance was measured at 652 nm, corresponding to the La–Arsenazo III complex, while the peak of the free dye at 535 nm was also monitored. As La concentration increased, the free dye absorbance at 535 nm decreased consistently. To ensure accurate quantification over a broad range, two calibration curves were prepared, one for low concentrations (15–500 ppb) and another for higher concentrations (15–1000 ppb), using different dye volumes. Each calibration curve yielded correlation coefficients (R^2) above 0.995.

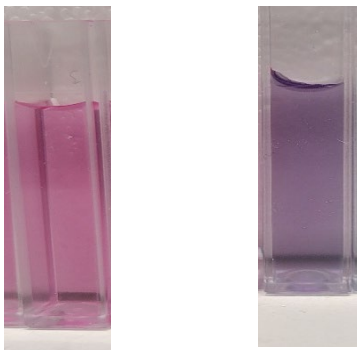

15 ppb 750 ppb

Figure 2-11. Representative calibration samples

The structural and surface characterisation of sorbents was performed using several complementary techniques. Nitrogen adsorption–desorption isotherms were obtained with a Micromeritics ASAP 2020 analyser to determine BET surface area, total pore volume, and average pore diameter. Scanning electron microscopy (SEM) was conducted using a Zeiss EVO MA10 microscope, and energy-dispersive

X-ray spectroscopy (EDX) was used to map elemental composition across the surface. Thermogravimetric analysis (TGA) was performed in a nitrogen atmosphere at a heating rate of 10 °C/min to 800 °C to evaluate the organic loading and thermal stability of grafted ligands or polymeric coatings. These techniques followed methodologies commonly applied in previous studies on functionalised silica and PBz-based sorbents.

In membrane separation experiments, losses of organic extractants were quantified by measuring total phosphorus (TP) and total organic carbon (TOC). Total phosphorus was used as a proxy for D2EHPA leakage and was determined using ICP. TOC analysis was performed on a Trace Elemental analyser in non-purgeable organic carbon (NPOC) mode. Before analysis, all samples were filtered through 0.45 µm syringe filters and acidified to a pH of less than 2. These measurements enabled evaluation of extractant retention and the overall stability of the liquid membrane.

Additional parameters, including pH, conductivity, and system pressure, were monitored throughout the experiments. pH measurements were conducted using WTW 3310 meters equipped with SenTix electrodes, calibrated using standard buffer solutions. Conductivity was tracked during selected membrane tests to observe acid back-diffusion and changes in ionic strength. Pressure sensors were installed on both feed and strip sides of the membrane unit to detect pressure drops and potential fouling, as recommended in earlier HFSLM assessments (Kim et al., 2016).

2.4 Life Cycle Based Risk and Opportunity Mapping

A sustainability assessment of the HFSLM technology was conducted using Life Cycle Based Risk and Opportunity Mapping (LCBROM), a qualitative screening approach developed to evaluate the environmental implications of emerging technologies at low Technology Readiness Levels (TRL). The LCBROM approach systematically examines potential risks and opportunities across all life cycle stages—production, use phase, and end-of-life—through a structured MET matrix framework that evaluates **M**aterials use, **E**nergy consumption, and **T**oxicity issues.

The assessment followed a six-step iterative procedure that involved close collaboration among technology developers, problem owners, and LCA experts. Initial stakeholder mapping identified key actors and expertise areas, followed by

questionnaire-based information gathering to document problem definitions, benchmark technologies, and case-specific parameters. A comprehensive literature review was conducted to evaluate existing life cycle assessments of the benchmark technology (solvent extraction), focusing on environmental hotspots and data quality limitations.

Stakeholder meetings were held to systematically populate the MET matrix, discussing both risks and opportunities while identifying knowledge gaps requiring further investigation. Risk mitigation measures and improvement opportunities were documented and evaluated. Throughout the process, findings were continuously updated in a structured report template, with significant observations tagged using standardised abbreviations (FX for findings, AX for assumptions) and cross-referenced within the MET matrix.

The methodology incorporates uncertainty management through standardised notation, where results with particularly high uncertainty are presented in italic font. Data gaps are explicitly identified, and colour-coding distinguishes between opportunities (green), risks (red), and areas requiring further assessment (yellow). This systematic approach enables early-stage identification of potential "bottlenecks" or "showstoppers" that could hinder technology development and scale-up. The inclusion of human health and environmental evaluations at low TRL also allows for the development of safer and more sustainable innovations.

3 Results and discussion

The experimental work was organised around three main stages of REE recovery: (1) the removal of undesired substances from aqueous matrices, (2) the pre-concentration of REEs using sorbent materials, and (3) the selective separation and up-concentration of REEs via hollow fibre-supported liquid membranes (HFSLM). These stages reflect the modular treatment approach outlined in the conceptual design (Figure 1).

Each stage involved several experimental campaigns conducted under varying conditions, including tests with synthetic and real mine waters, different pH levels, varying contact times, and different flow configurations. A variety of analytical methods were used to monitor REE concentrations, interfering elements, and operational stability, as described in Section 2.4. Wherever possible, experiments were designed to generate comparative data across different materials or setups, thereby supporting an integrated assessment of system performance.

3.1 Removal of undesired substances

Electrocoagulation (EC) was evaluated as a first-stage pre-treatment for mine water from Lovisagruvan spiked with 10 µg/L each of Y, La, Nd and Dy. Aluminium electrodes operating at 120 A/m² generated in situ $Al(OH)_3$ flocs that adsorbed transition metals, while ideally allowing trivalent lanthanides to remain in solution. Seven batch trials were performed with inlet pH values ranging from 4.8 to 8.1 (Table 2-1 in Section 2.1).

Initial analysis of the spiked mine water revealed lower REE concentrations (2.6-3.35 µg/L) than expected, compared to the target of 10 µg/L, suggesting partial adsorption losses during sample preparation. After acidification to pH 4.8 and filtration, REE concentrations stabilised at 2.3-3.3 µg/L, which served as the baseline for evaluating EC performance.

Table 3-1 presents the complete dataset, showing metal concentrations before and after EC treatment at all tested pH conditions.

Table 3-1. Metal concentrations (µg/L) before and after electrocoagulation at different inlet pH values, with reduction percentages.

Element	Y	La	Nd	Dy	Zn	Pb	Cd
Untreated feed	3.35	2.85	2.6	2.75	915	40.5	11
pH 4.8 (outlet 7.6)	3.3	2.6	2.2	2.3	190	8.7	2.3
Reduction (%)	1%	9%	15%	16%	79%	79%	79%
pH 5.5 (outlet 7.5)	0.15	0.15	0.14	0.13	16	1.4	0.39
Reduction (%)	96%	95%	95%	95%	98%	97%	96%
pH 6.9 (outlet 7.8)	0.24	0.24	0.21	0.21	15	1.1	0.42
Reduction (%)	93%	92%	92%	92%	98%	97%	96%
pH 8.1 (outlet 8.3)	0.055	0.047	0.043	0.046	2.4	0.12	0.038
Reduction (%)	98%	98%	98%	98%	100%	100%	100%

At the lowest inlet pH (4.8), the EC process demonstrated remarkable selectivity, with approximately 79% of zinc, lead, and cadmium being removed. In comparison, 84-99% of the REEs remained in solution, representing an enrichment factor of 5- to 80-fold for REEs relative to these transition metals. As the inlet pH increased to 5.5, selectivity was lost, with both REEs and transition metals showing greater than 95% removal. At pH 8.1, near-complete precipitation of all metals occurred, confirming that alkaline conditions are unsuitable when REE enrichment (rather than total removal) is the objective.

Several transition metals, notably Fe, Cr, and Cu, exhibited unexplained concentration increases after the initial acidification of the raw sample, but these increases were reversed after EC treatment. This anomalous behaviour may result from the dissolution of particulate matter during acid pre-adjustment, with subsequent capture by $Al(OH)_3$ flocs at higher pH levels. Strontium and barium remained largely unaffected by EC treatment, consistent with their weak affinity for aluminium hydroxide. Molybdenum similarly showed minimal removal, reflecting its anionic speciation at circumneutral pH.

3.1.1 Selectivity and enrichment

The data demonstrate that EC functions as a practical pre-concentration step when operated at acidic inlet pH. At pH 4.8-5.0, the process selectively removes divalent

transition metals (Zn^{2+}, Pb^{2+}, Cd^{2+}) while retaining trivalent lanthanides in solution. This pH-dependent selectivity can be attributed to the differential complexation behaviour of these metal groups with aluminium hydroxide flocs. The resulting solution contains REE/transition-metal ratios enriched by up to two orders of magnitude, substantially reducing the burden on downstream sorption or membrane extraction stages.

3.1.2 Process implications

Because EC employs only electricity and consumable aluminium electrodes—materials readily available at mine sites—it represents a low-cost, chemical-free pre-treatment option for processing large volumes of low-grade water. The process requires no external chemical addition beyond initial pH adjustment and generates a manageable aluminium hydroxide sludge that can be disposed of using existing mine waste management infrastructure.

The sharp transition in selectivity between pH 4.8 and 5.5 suggests that precise pH control is critical for successful implementation. Future optimisation should focus on maintaining inlet pH in the narrow 4.8-5.2 window to maximise REE retention while meeting regulatory discharge limits for Zn and Pb. Integration with downstream processes must account for the acidic nature of the EC effluent, which may require neutralisation before certain sorption or membrane stages.

3.2 Sorption performance of functionalised sorbents

This section presents the comparative performance of various functionalised sorbents for the up-concentration of rare earth elements (REEs) from solution. By evaluating a diverse set of materials—including functionalised silica, lignin-based composites, and poly-benzoxazine (PBz) carbons—under controlled experimental conditions, the results provide insight into the sorption capacities and selectivity of each sorbent.

3.2.1 Comparative isotherm analysis

Six sorbents—three silica-based, one lignin composite and two poly-benzoxazine (PBz) carbons—were benchmarked for La^{3+} uptake under identical solution chemistry. Equilibrium data (1–30 mg/L) followed Langmuir behaviour for the silica and carbon materials and a Freundlich response for the lignin composite. The complete set of isotherm constants is presented in Table 3-2, while Figure 3-1 gives a representative overlay of experimental and modelled curves.

Table 3-2. Langmuir and Freundlich parameters and statistics for La^{3+} on functionalised silica, lignin composite, PBz-modified carbons and AAC carbon materials

Sample	Langmuir model				Freundlich Model			
	Q_m (mg/g)	K_L (L/mg)	R^2	Chi-sq. (χ^2)	K_F [(mg/g)(mg/L)1/n]	1/n	R^2	Chi-sq. (χ^2)
SiAP	55.12	87.42	0.95	7.69	47.35	0.08	0.82	31
D2-SiAP	30.23	254.07	0.94	0.21	28.77	0.024	0.86	0.51
DG-SiAP	23.14	111.41	0.9	0.16	21.96	0.08	0.82	31
ZLC	5.1	2.2	0.95	0.04	3.71	0.55	0.98	0.01
DPABz AC	10.6	4.62	0.96	0.91	5.49	0.179	0.81	4.73
PhPhBz AC	9.12	4.93	0.94	1.02	5.05	0.152	0.68	5.78
Raw AC	12.93	1.7	0.93	2.46	5.84	0.211	0.75	7.26
AAC-1	69.13	0.16	0.97	6.12	1.01	0.51	0.96	15.3
AAC-2	80.52	0.12	0.95	5.57	0.51	0.43	0.90	13.1

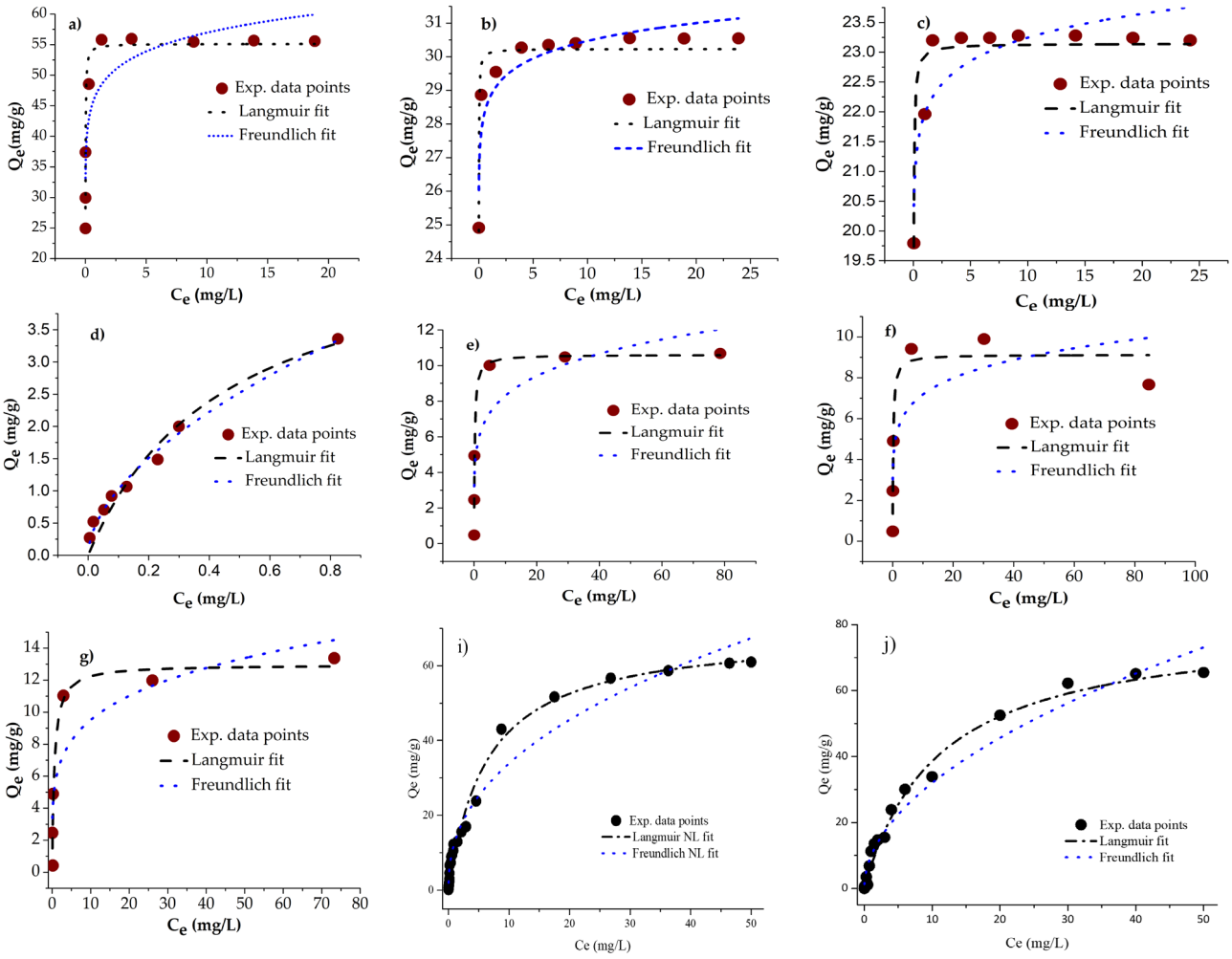

Figure 3-1. Overlay of experimental isotherms and Langmuir and Freundlich fits for all six sorbents (a:SiAP; b: D2-SiAP; c: DG-SiAP; d: ZLC; e: DPABZ AC; f: PhPhBZ AC; g: Raw (Ecosorb) AC)

SiAP (amine-grafted silica) provided the highest monolayer capacity, confirming that primary amines give the densest accessible binding surface; its affinity coefficient, though moderate, is adequate for mg/L feeds. Impregnating the same scaffold with D2EHPA (D2-SiAP) sacrificed roughly half the capacity but tripled affinity—an advantageous trade-off when treating sub-µg/L concentrations. The diglycolamide variant (DG-SiAP) offered the lowest capacity among the silicas and an intermediate affinity; its plateau at high concentration suggests diffusion-limited access to the DGA pockets.

PBz-modified carbons, although an order of magnitude lower in capacity than SiAP, exhibited respectable affinities and a markedly different surface chemistry. The DPA-derived PBz (DPABz AC) outperformed the commercial Ecosorb carbon in affinity, consistent with the stronger donor character of its carboxylated

benzoxazine, while the phenolic PBz (PhPhBz AC) balanced capacity and affinity. The zwitterionic lignin/chitosan composite (ZLC) exhibited the most heterogeneous surface—Freundlich $R^2 = 0.98$—and tolerated wider pH excursions; however, its capacity was only 5 mg/g, indicating that it should be deployed either as a polishing medium or in matrices where its renewability outweighs loading constraints.

The adsorption data for samples AAC-1 and AAC-2 can be better explained by the Langmuir empirical adsorption model, which suggests that adsorption occurs in a single layer on the surface of the biochar, characterised by a finite number of active sites. Q_m represents the theoretical maximum amount of material that can be adsorbed by the adsorbent when the adsorbate has covered all the active sites. K_L is a Langmuir model constant and is related to the affinity between the adsorbate and the adsorbent. A higher K_L value indicates a stronger binding affinity. AAC-1 (K_L 0.16 L/mg, Qm 69.13 mg/g) relates to a relatively stronger binding affinity than AAC-2 (K_L 0.12 L/mg, Qm 80.52 mg/g), but a lower number of total sites.

3.2.2 Adsorption kinetics

Kinetic tests, modelled with the pseudo-second-order (PSO) equation, corroborate these equilibrium trends. A representative fit for SiAP appears in Figure 3-2; PSO constants for all sorbents are summarised in Table 3-3.

Table 3-3. PSO kinetic parameters (1 mg/L La^{3+})

	SiAP	D2-SiAP	DG-SiAP	ZLC	DPABz AC	PhPhBz AC
Qe (mg/g)	5.0	4.2	4.9	1.9	2.6	2.4
k2 (g/mg min)	0.20	0.22	0.005	0.011	0.035	0.030
Half-time $t_{0.5}$ (min)	3	4	60	45	22	25

SiAP and D2-SiAP attained 75% of equilibrium loading within fifteen minutes, making them suitable for short-contact fixed beds. DG-SiAP, by contrast, required roughly one hour to reach half-loading, limiting its practicality to batch polishing unless its pore connectivity is improved. Both PBz carbons and ZLC exhibited intermediate half-times (22–45 min), which is acceptable for column empty-bed contact times of 30–60 min. The conductive PBz matrix also enables electro-desorption, potentially lowering chemical regeneration costs in continuous operation.

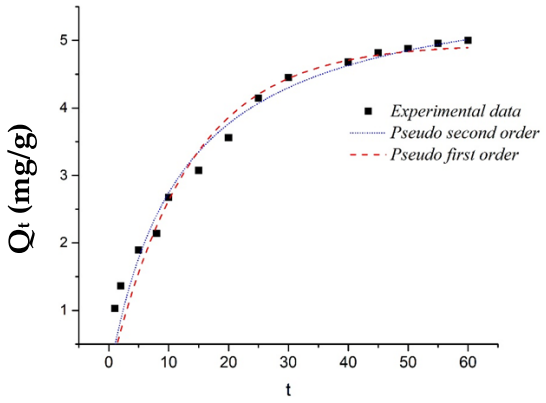

Figure 3-2. Pseudo-second-order fit for La^{3+} adsorption on SiAP (1 mg/L, sorbent dose 0.2 g/L, pH 5.5).

3.2.3 Key comparative insights

In summary, silica sorbents dominate where capacity or rapid kinetics are paramount, PBz carbons offer electro-swing regeneration and moderate tolerance to hardness ions, and ZLC provides a renewable option for alkaline or fluctuating pH conditions. Selecting among these materials, therefore, depends less on intrinsic uptake numbers than on process context: SiAP for compact columns at low pH, D2-SiAP for trace-level polishing, DG-SiAP for batch reservoirs, PBz carbons for electro-regenerable beds, and ZLC for sustainable treatment of high-alkalinity waters.

3.3 Separation and up-concentration of REEs using HFSLM

The hollow-fibre supported liquid membrane (HFSLM) pilot was operated in a series of campaigns that differed in feed matrix, pH, hydraulic mode and operating time. Results are presented below in the order most relevant to process design: overall transport behaviour and selectivity, the influence of operating parameters, membrane stability and finally implications for scale-up.

3.3.1 Influence of pH and zinc

Feed pH emerged as the dominant operating parameter, controlling both extraction kinetics and membrane stability. Semi-circulation trials with 50 L of synthetic feed containing 25 mg/L each of La, Nd, Y and Dy revealed three distinct transport regimes corresponding to pH ranges of 1.0–1.5, 1.5–2.0 and 2.0–3.0. Results are shown in Figure 3-3.

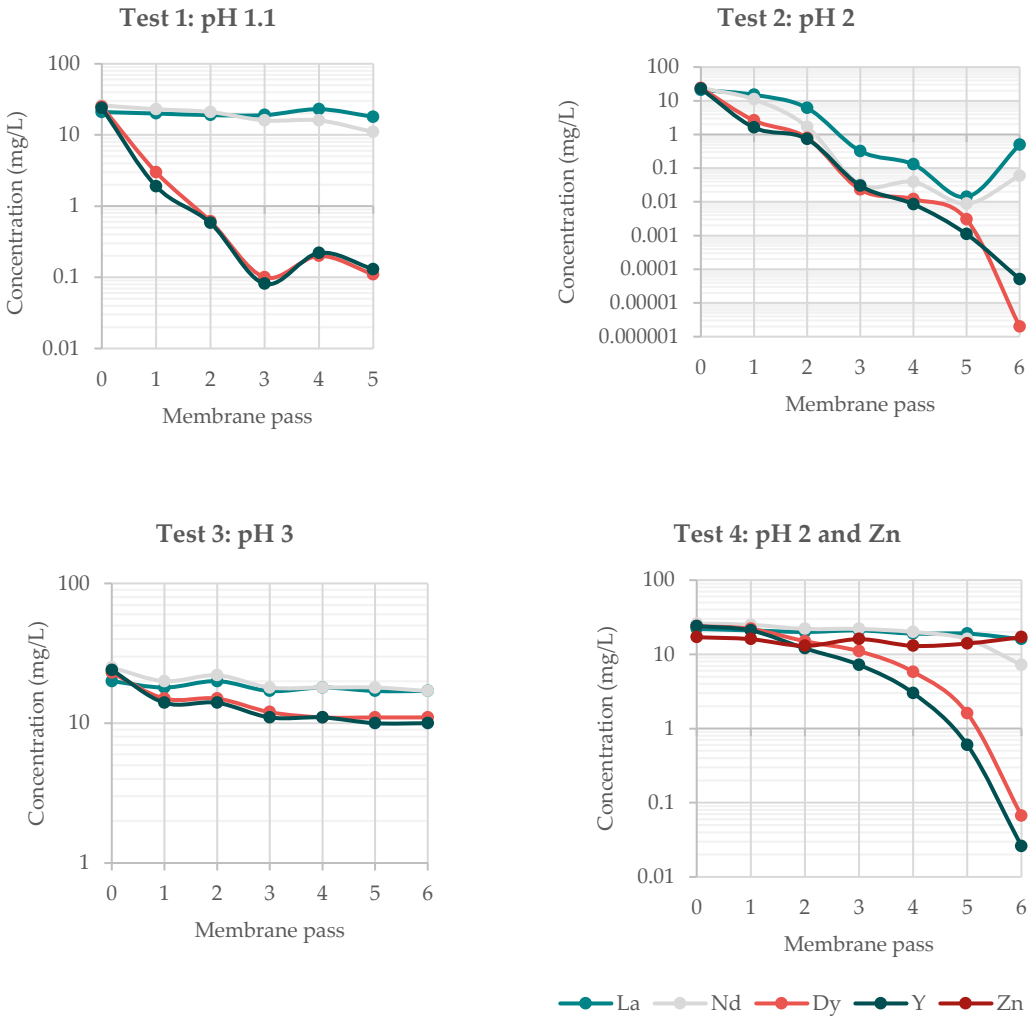

Figure 3-3. REE concentration profiles in feed tank during semi-circulation trials at different pH values. Four panels showing: (a) Test 1 at pH 1.1, (b) Test 2 at pH 2.0, (c) Test 3 at pH 3.0, and (d) Test 4 at pH 2.0 with zinc addition.

At pH 1.1 (Test 1), heavy REEs (Y, Dy) showed rapid initial extraction, achieving near-complete removal within the first membrane pass. Light REEs (La, Nd), by contrast, exhibited minimal transport until the feed pH was adjusted to 1.8 after multiple passes, allowing for complete extraction. This observation is in accordance with the selectivity inversion (not a reversal of the extraction order, but a shift in the dominant factor controlling that order), where proton competition dominates over ionic radius effects below pH 1.5.

The best transport occurred at pH 2.0 (Test 2), where all four REEs reached >90% removal within three passes. Feed-side depletion followed the expected order: Y

and Dy > Nd and La, consistent with literature distribution ratios for D2EHPA/kerosene systems (Martínez et al., 2018).

Strip-side accumulation in 5 L strip solution at pH 2 was 540 mg La after one pass, 820 mg Nd, 700 mg Dy and 790 mg Y, corresponding to 43 %(La), 66 %(Nd), 56 %(Dy) and 64 %(Y) of total amounts in the feed, representing a 20-30-fold concentration factor. However, unexpectedly, the number of passes decreased the amount of REE in the strip solution. After three passes, the recovery was 34% for La, 50% for Nd, 39% for Dy, and 63% for Y. The reason for this is not explained, and it is contradictory because the concentration at the feed side decreases between each pass.

Increasing the feed pH to 3.0 (Test 3) triggered gel formation visible as white precipitates in the feed tank (Figure 3-4). REE transport rates declined sharply. The gel, tentatively identified as polynuclear hydroxo-REE-phosphate complexes, adhered to fibre walls and resisted dissolution in fresh acid.

Figure 3-4. Photograph of gel formation during Test 3 at pH 3.0, showing white precipitates in the strip tank.

The addition of Zn (17 mg/L, Test 4) at pH 2.0 resulted in minimal co-transport of Zn, with approximately 20% observed after five passes and less than 5% after six passes. The gel formation from Test 3 likely decreased performance compared to Test 2, where membranes worked well. The selectivity, however, with separation factors exceeding 20 for each La over Zn, confirms that D2EHPA maintains its affinity hierarchy even at elevated Zn:REE ratios typical of mine water drainage. A

summary of REE removal efficiencies and selectivity at different feed pH values is provided in Table 3-4

Table 3-4. Summary of REE removal efficiencies at the feed side and transport selectivity at different feed pH values after five passes.

Test	Feed pH	La Removal (%)	Nd Removal (%)	Y Removal (%)	Dy Removal (%)	Zn Removal (%)	Key Observation
1	1.1	14.3%	57.7%	99.6%	99.5%	—	Heavy REE selectivity
2	2.0	99.9%	100.0%	100.0%	100.0%	—	Optimal transport
3	3.0	15.0%	28.0%	52.2%	58.3%	—	Gel formation
4	2.0	13.6%	38.5%	93.3%	97.5%	17.6%	No or low Zn interference

3.3.2 Matrix effects: mine-water versus tap-water feeds

A direct comparison of tap water and mine water matrices revealed that real wastewater components had a minimal impact on REE extraction performance, provided adequate pre-treatment was applied. Three sequential trials—synthetic reference, mine water, and synthetic reference repeat—quantified matrix tolerance under identical operating conditions (pH 1.25-1.3, 180 L/h feed, 1 M HCl strip) and total volume of 50 L.

The initial reference test with tap water spiked to 1.8 mg/L Y achieved 96% removal after three passes, with outlet concentrations decreasing from 1.8 to 0.019 mg/L. Mining water from Lovisagruvan mine, adjusted to the same pH and spiked with 0.49 mg/L Y, showed comparable extraction kinetics despite containing millimolar levels of Ca^{2+}, Mg^{2+}, SO_4^{2-}. The removal efficiency reached 98% under identical residence times.

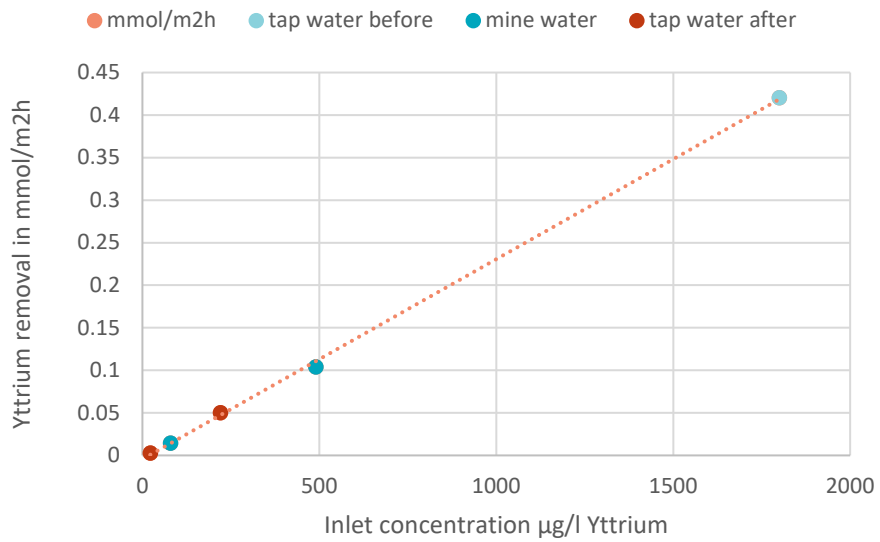

Figure 3-5. Y removal efficiency comparison between tap water and mine water matrices.

The second reference test, conducted immediately after the mine water trial, exhibited equal performance, with a Y removal of 98%. Table 3-5 compares the feed water composition and extraction performance for the matrix comparison trials

Table 3-5. Feed water composition and extraction performance for matrix comparison trials

Parameter	Tap Water Reference 1	Mine Water	Tap Water Reference 2
Initial Y (mg/L)	1.8	0.4	0.2
pH	2.0	2.0	2.0
Ca^{2+} (mg/L)	<1	250	<1
SO_4^{2-} (mg/L)	<10	1200	<10
TOC inlett (mg/L)	5.3	1.7	<11
TOC outlet 3 pass(mg/L)	20	11	n.m, but 11 after pass 1
Y removal 3 passes(%)	**96**	**98**	**98**
Fe in strip (mg/L)	<0.1	0.5	0.5

The mine water matrix introduced no detectable REE-complexing agents or competitive extractants, as evidenced by unchanged pH profiles and consistent extraction rates. Total organic carbon remained below 20 mg/L, and the loss of P was always lower than 15 µg/L throughout, well within the tolerance window

established in preliminary trials. P measurements indicate a total loss of D2EHPA to the Feed solution of less than 0.03% of the total D2EHPA.

ICP-MS analysis of the strip solution revealed trace Fe accumulation (0.5 mg/L) that persisted despite intermediate water flushing. This Fe, originating from corrosion during earlier HCl trials, apparently formed mixed complexes with D2EHPA. A long-term circulation test with 1000 L of 5 mg/L Y resulted in a gel forming at the strip side, which partially blocked the pump.

3.3.3 Membrane stability

Long-term membrane stability was evaluated through a 16-day continuous campaign and multiple regeneration cycles. Extractant loss, quantified via total phosphorus (TP) and total organic carbon (TOC) measurements in an earlier test in 2023, averaged 0.03% of the initial D2EHPA inventory per day under steady-state conditions for one long-time test with 900 L of tap water with Zn, where pH in feed was kept at 2.8.

In experiments where 280 mg of phosphorus was dissolved in 900 L of feed water over 20 hours, there was an estimated loss of about 3 g of D2EHPA from the initial 30 g loading. The observed loss of TOC was comparatively lower than that of D2EHPA, with an increase of 2 mg/L TOC, totalling 2 g. In separate trials using mining water and tap water, with 1 mg/L of Y added to a 50 L feed at pH 1.2-1.3 and processed through the membrane three times in semi-continuous mode, the measured D2EHPA loss was less than 8 mg per trial. The difference likely stems from variations in pH, with the dissolution of D2EHPA being more pronounced at higher pH levels in the feed water. A summary of the membrane degradation and regeneration results is presented in Table 3-6.

Table 3-6. Membrane degradation and regeneration summary

Parameter	Initial	After pH 3 event	After 7 days	After 16 days	Post-regeneration
H^+ back-diffusion (mmol/min)	0.20	>10	3.6	0.06(1)	0.22
Strip flow rate (L/h)	75	75	30	5(2)	73
Flux recovery (%)	100	60	40	<10	95

(1) With continuous stirring
(2) Due to gel formation

For the long-term test, hydrogen with tap water back-diffusion served as a sensitive indicator of membrane integrity. Initial rates of 0.20 mmol/min increased to 3.6 mmol/min in periods where only tap water was added, reflecting the possible dissolution of the membrane that can occur due to mechanical abrasion and the dissolution of D2EHPA at higher pH levels. Following the pH 3 gelation event, back-diffusion surged to unmeasured levels, confirming loss of phase separation. Remarkably, continuous stirring of the strip solution with suspended kerosene droplets (at a 1:25 volume ratio) progressively restored membrane function over 4–7 days, reducing H^+ leakage to near-baseline values. The effect of different HCl concentrations on Zn removal is illustrated in Figure 3-6.

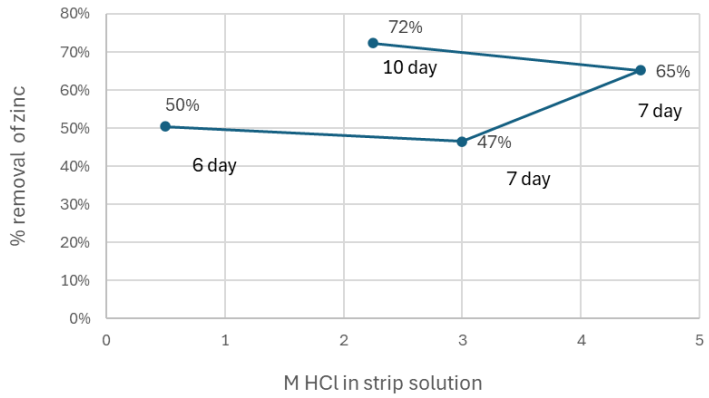

Figure 3-6. Zn removal at four different stripping concentrations of HCl (0.5 M, 2.25 M, 3M and 4.5M) over D2EHPA/kerosene membrane. Feed concentration 149 mg zinc/l, 120 L/h feed flow,

Strip acid concentration emerged as a critical stability parameter. Tests with 0.5–4.5 M HCl revealed an unexpected peak for the Zn removal at 2.25 M, where Zn removal efficiency reached 72%—significantly higher than at either 0.5 M (50%) or 4.5 M (65%). The reasons for this non-monotonic response are not fully understood. It is possible that intermediate acid strength could help balance stripping kinetics with extractant protonation, thereby limiting excessive phase disruption. Additionally, the relatively higher removal rate observed could be partially attributed to the duration of stirring; after 10 days of emulsion agitation, membrane formation appears to be more efficient, possibly due to some level of membrane recovery.

The most severe degradation occurred during the 1000 L Y trial, where 5 g Y was added to 1000 L of tap water and the pH was maintained at 2.0. Under these conditions, D2EHPA-kerosene transformed into a viscous, yellow-brown gel after 3–7 days. This material, containing polymerised Y-P complexes or possible Y-P-Fe

complexes, reduced strip flow from 75 to 5 L/h and ultimately destroyed the pump tubing. Adding fresh extractant (400 mL of 10% D2EHPA in kerosene) temporarily restored function, but the gel reformed within a few days. Fe contamination (0.5 mg/L in strip) likely catalysed this polymerisation, as similar degradation was not observed in iron-free trials. Figure 3-7 shows the visual progression of extractant degradation during long-term operation.

Successful regeneration required complete module drainage, ethanol washing (96%, 5 L), air drying (24 h at 27°C), and re-impregnation with fresh extractant. This protocol, performed four times during the study, consistently restored more than 95% of the initial flux and maintained hydrophobicity, as verified by 4-bar pressure tests.

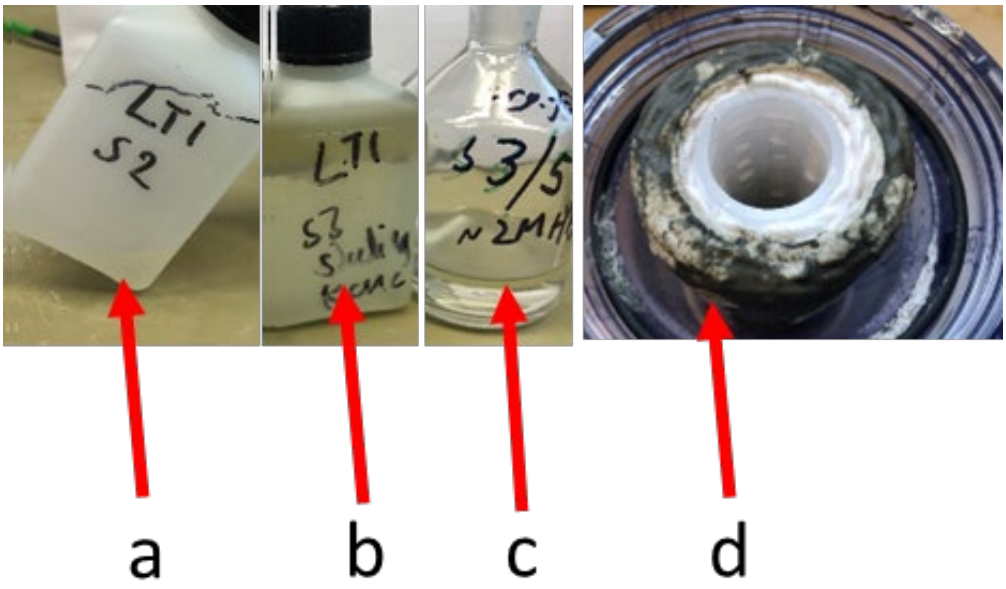

Figure 3-7. Visual progression of extractant degradation: (a) LT1 S2 strip solution after 2 days run under normal operationno gel formation (b) strip solution with yellow-brown gel formation after 7 days run, LT1S3, (c) kerosene mixture after 7 days that was leached with strong acid for 2 month LT1S3/5 (d) Viscous material blocking pump and also transported into the feed penetrating into the prefilter in feed solution after 3-10 days

3.3.4 Literature comparison

The operating envelopes reported here—feed pH 1.3-2.0, strip 1.5 M HNO_3, 10 vol% D2EHPA in kerosene, flow rates of 180 L/h (feed) and 75 L/h (strip)—represent a significant scale-up from typical laboratory studies, while maintaining performance comparable to that of smaller systems. Table 3-7 benchmarks the present pilot against four representative HFSLM studies, demonstrating that this work achieves the highest throughput reported for dilute feeds (<50 mg/L total

REE). Table 3-7 benchmarks the present pilot against representative HFSLM studies from the literature.

Table 3-7. Operating envelope for HFSLM extraction – present work vs. representative literature.

Parameter (range)	This study (pilot)	KTH bench pilot[1]	(Wannachod et al., 2015)	(Ni'am et al., 2020)	(Li et al., 2022)
Feed/strip flow (L/h)	180/75	30/30	0.1 / 0.1	90 / 90	Flat sheet
Feed pH (optimum window)	1.3 – 2.0	1.5 – 2.0	4.5 (Nd)	2.0	3.0 (range 2-4 tested)
Extractant & concentration	10 vol% D2EHPA in kerosene	10 vol% D2EHPA	0.5 M PC88A / octane	1 M D2EHPA / Isopar L	5% (v/v) 507P in D80
Strip acid (mol/L)	1.5 HNO_3 [2]	3 HCl	3 M H_2SO_4	2 M HNO_3	3M HCl
Key outcome	80–90% La/Nd recovery; 12× conc. factor	High SF at high conc.	98% Nd extraction	58.62% Nd recovery in 35 min; selective separation from Fe	91% Nd recovery; Nd/La selectivity 44.25; anion transformation

(1) Bench pilot data from KTH–IVL collaboration 2012–2018.
(2) Tests with 0.5–4.5 M HCl were also performed for the hydrodynamic study.

The current pilot operates at flow rates 1800-fold higher than those of Wannachod et al. (2015), who used 0.1 L/h in laboratory-scale experiments, and 6-fold higher than the KTH bench pilot (30 L/h). Despite this scale-up, the system maintained an 80-90% recovery rate for La and Nd with a 12-fold concentration factor, comparable to or exceeding the results of smaller-scale studies.

Notable differences in operating conditions reflect both scale effects and process optimisation strategies. While Wannachod et al. achieved 98% Nd extraction at pH 4.5 using PC88A extractant, the present study deliberately operated at lower pH (1.3-2.0) to prevent gel formation—a critical operational constraint identified during long-term trials. Similarly, Ni'am et al. (2020) reported 58.62% Nd recovery at pH 2.0, demonstrating that moderate pH operation represents a practical compromise between extraction efficiency and membrane stability.

The Li et al. (2022) study, which employs a flat-sheet configuration instead of a hollow-fibre configuration, provides a valuable comparison for selectivity

performance. Their Nd/La separation factor of 44.25 exceeds values observed in the present work, suggesting that membrane geometry and hydrodynamics significantly influence selectivity beyond simple extractant chemistry.

Building on insights from Alemrajabi et al. (2022), this pilot study refined operational protocols in two key areas. First, systematic comparison of HNO_3 versus HCl as strip acids revealed superior long-term stability with nitric acid, despite slightly lower stripping kinetics. Second, the gel formation issue at pH ~3—particularly problematic for Y extraction—was successfully managed through periodic rejuvenation of the strip solution with fresh acid and supplemental D2EHPA additions, thereby avoiding the need for complete membrane replacement, which would be impractical at an industrial scale.

The ability to maintain continuous operation for 16 days at pilot scale, processing feed volumes exceeding 1000 L, represents a critical advancement toward industrial implementation. This duration exceeds most reported HFSLM studies and provides essential data on extractant degradation, membrane fouling, and regeneration requirements that cannot be obtained from short-term laboratory experiments.

3.3.5 LCBROM results

Environmental Performance Comparison

LCBROM assessment reveals that HFSLM technology addresses key environmental challenges associated with conventional solvent extraction while introducing specific sustainability considerations. A literature analysis of solvent extraction processes identified hydrochloric acid consumption as the dominant environmental impact contributor, with industrial operations requiring 0.28-6.96 kg HCl per kilogram of REO due to a high stoichiometric excess. The current HFSLM configuration theoretically requires approximately 1 kg HCl/kg REE, like solvent extraction, but with potential for more optimised consumption without stoichiometric excess.

Material inventory analysis demonstrates significant advantages for HFSLM implementation. The technology requires substantially lower organic extractant volumes compared to mixer-settler operations, with the pilot study utilising 30 g of D2EHPA loading, versus industrial solvent extraction circuits that require tons of organic phase inventory. However, membrane degradation introduces periodic

replacement requirements, with observed extractant loss averaging 0.03% per day under steady-state conditions.

Resource Efficiency and Waste Stream Management

The hollow fibre membrane system generates distinct waste streams that require specialised management protocols. Membranes containing polypropylene fibres, polyethene potting, and Viton gaskets present opportunities for material recovery through established plastics recycling pathways. However, extractant-contaminated membranes require appropriate hazardous waste handling due to D2EHPA and kerosene residuals.

Process liquid waste streams differ qualitatively from conventional solvent extraction, with lower total organic volumes but concentrated acid solutions containing dissolved REE traces. The regeneration protocol involving ethanol washing generates additional organic waste streams, although the volumes remain significantly lower than those of comparable mixer-settler operations.

Toxicity and Occupational Health Considerations

A workplace risk assessment conducted during pilot-scale operation identified manageable exposure risks for laboratory conditions, with most hazards reducible to low-risk levels through the implementation of appropriate engineering controls. However, industrial-scale implementation will require enhanced safety protocols due to increased chemical inventories and process intensification. The technology maintains similar extractant chemistries to conventional processes (D2EHPA, kerosene) but at substantially reduced volumes, proportionally decreasing exposure potential while maintaining inherent chemical hazards.

3.3.6 Process implications and scalability

Pilot trials demonstrated that HFSLM technology achieved a one to two orders of magnitude reduction in solvent inventory compared to literature values for mixer-settler circuits (Binnemans et al., 2013); however, direct comparative data under identical conditions were not generated. The compact footprint—approximately 10 times smaller than equivalent mixer-settlers based on module dimensions—comes with operational constraints: strict pH control (<3 to prevent gel formation, <2 for optimal performance), sensitivity to zinc interference (>10 mg/L affects extraction), and undefined DOC tolerance, requiring further investigation.

The one-month pilot campaigns established three critical control parameters: (i) feed pH maintained below 2 for stable operation, (ii) zinc concentration requiring

monitoring and potential pre-treatment above 10 mg/L, and (iii) extractant loss managed through ethanol-based regeneration cycles every 2-3 weeks. Total phosphorus and pressure drop measurements provided a 24-48 hour warning of membrane degradation, with TP increases exceeding 20% indicating the need for imminent intervention.

Membrane lifetime beyond one month remains unverified, presenting uncertainty for industrial design, where module replacement costs could be significant. While polypropylene hollow fibres theoretically offer recycling potential, extractant contamination pathways and disposal protocols require further development. The study did not quantify acid consumption rates, which prevented comparison with industrial mixer-settlers, where a 20-50% stoichiometric excess is typical.

Kerosene diluent, while standard in solvent extraction, may face regulatory restrictions at an industrial scale. Alternative diluents require systematic evaluation for extraction efficiency, membrane compatibility, and long-term stability—work not undertaken in this study. Gel formation between Y and D2EHPA, observed at pH levels greater than 3, represents an unresolved operational risk that requires either chemical modification or process control strategies.

Rather than speculative hybrid configurations, scale-up should focus on demonstrated capabilities, such as extending proven one-month operations to 3-6 months, quantifying actual solvent and acid consumption under continuous operation, and validating performance with varying feed compositions. Industrial implementation requires the resolution of membrane durability issues and the development of standardised replacement protocols before economic viability can be assessed. The technology shows promise for specific applications—particularly low-volume, high-value REE streams—but claims of general scalability require substantial additional validation.

Further development should focus on extractants with lower solubility in acidic media, alternative fibre chemistries that resist wetting, and hybrid process trains that couple selective electro-sorption with membrane extraction to handle fluctuating compositions typical of mine-water effluents. Additionally, it is crucial to find a method to minimise gel formation of REE and extractants, such as those observed for Y and D2EHPA. Continuous monitoring of TP and pressure drop proved to be reliable early-warning indicators of membrane degradation and should be incorporated into any scale-up scenario.

4 Conclusions

This study has demonstrated the technical feasibility of extracting rare earth elements from dilute mining waters using an integrated process combining pre-treatment and hollow fibre supported liquid membrane (HFSLM) technology. The pilot-scale trials provide important proof-of-concept data, though several critical aspects require further investigation before commercial viability can be established.

Technical achievements

- HFSLM technology successfully extracted REEs from real mine water containing concentrations of ng/L to µg/L at pilot scale, achieving a recovery efficiency of over 90% under controlled conditions (pH < 3).
- pH-controlled selective separation of individual REEs was demonstrated, showing the ability to differentiate between elements tested, though more complex real-world matrices may require additional optimisation.
- Bench-scale testing of functionalised sorbents showed promising selectivity for iron and aluminium removal, with SiAP demonstrating a capacity of 45 mg/g.
- One-month continuous operation was achieved without significant membrane failure, providing a reference for operational protocols.
- Matrix effects from real mine water were manageable, with no significant interference observed compared to synthetic feeds.

Key limitations identified

- Membrane stability beyond one month remains unverified, with extractant durability identified as a primary constraint to this stability.
- Separation of zinc from the lighter REE requires additional process considerations and is easiest solved with careful feed pre-treatment.
- The operating pH value is crucial in preventing gel formation, thereby necessitating pH control.
- Energy consumption for electrocoagulation pre-treatment may impact overall process economics.
- Sorbent performance demonstrated only at bench scale, requiring pilot-scale validation.
- No economic analysis was performed, preventing the assessment of commercial competitiveness.

Critical knowledge gaps

The study has not addressed several factors essential for industrial implementation:

- Absence of techno-economic analysis comparing costs with conventional solvent extraction.
- Lack of regeneration data for both sorbents and membranes over multiple cycles.
- Scale-up validation is necessary for promising sorbents to transition from bench to pilot-scale operations.
- Selective REE separation demonstrated under controlled conditions but requires validation in complex multi-element matrices.
- Environmental benefits claimed but not quantified through a comprehensive assessment.

While the integrated process shows technical promise for REE recovery from dilute streams, claims of commercial readiness would be premature. The technology is best characterised as TRL 4-5 (technology validated in a relevant environment), with individual components at different maturity levels - HFSLM at pilot scale, but sorbents still at bench scale. The demonstrated ability to selectively separate individual REEs through pH control represents an important advance, as does the one to two orders of magnitude reduction in solvent inventory compared to mixer-settlers. However, these achievements must be weighed against unresolved operational challenges and unknown economics.

The results provide a foundation for continued development. However, they should not be interpreted as establishing a commercially viable alternative to existing technologies without addressing the identified gaps in long-term stability, economic performance, and scalability.

4.1 Outlook

Progression toward industrial application requires systematic addressing of the identified limitations through the following prioritised activities:

Immediate priorities (6-12 months):

1. Scale up promising sorbents (particularly SiAP) from bench to pilot scale to validate performance.
2. Extend pilot campaigns to 3-6 months to establish the frequency of extractant replacement and determine actual operational costs.
3. Conduct a comprehensive techno-economic analysis, including CAPEX, OPEX, and a comparison with conventional routes, to the extent possible.

4. Further optimise pH control strategies for selective REE separation in complex, multi-element matrices.
5. Generate sorbent regeneration data over a minimum of 20 cycles.

Medium-term development (1-2 years):

1. Develop and evaluate an integrated continuous pilot treatment process based on a real case study, where potential tools such as EC, pilot-scale sorption columns, and HFSLM are combined and interconnected.
2. Evaluate environmentally benign alternatives to kerosene while maintaining extraction performance.
3. Investigate membrane recycling pathways and the incorporation of recycled polypropylene content.
4. Validate selective separation protocols for the full range of REEs in real mine water matrices.

Long-term validation (2-3 years):

1. Complete life-cycle assessment to substantiate environmental claims.
2. Demonstrate scalability through progressively larger pilots (10x, 100x current scale).
3. Establish partnerships with mining operations for extended field trials and testing.
4. Develop quality assurance protocols for separated REE products.

This research contributes valuable insights into membrane-based REE recovery from dilute streams, including the demonstration of selective individual REE separation through pH control. However, the technology should be positioned as an emerging approach that requires continued development, rather than a ready solution. The transition from bench-scale sorbent success to integrated pilot-scale operation represents a critical next step. Success will depend on addressing the economic and operational challenges identified herein, with a particular focus on demonstrating cost competitiveness and long-term stability. The compact footprint, reduced solvent inventory, and demonstrated selectivity remain compelling advantages that justify continued investigation, provided future work maintains a realistic assessment of both capabilities and limitations.

5 References

Alemrajabi, M., Ricknell, J., Samak, S., Rodriguez Varela, R., Martinez, J., Hedman, F., Forsberg, K., Rasmuson, Å.C., 2022. Separation of Rare-Earth Elements Using Supported Liquid Membrane Extraction in Pilot Scale. Ind. Eng. Chem. Res. 61, 18475–18491. https://doi.org/10.1021/acs.iecr.2c03268

Anyanwu, J.-T., Wang, Y., Yang, R.T., 2020. Amine-Grafted Silica Gels for CO2 Capture Including Direct Air Capture. Ind. Eng. Chem. Res. 59, 7072–7079. https://doi.org/10.1021/acs.iecr.9b05228

Basargin, N.N., Ivanov, V.M., Kuznetsov, V.V., Mikhailova, A.V., 2000. 40 years since the discovery of the arsenazo III reagent. J. Anal. Chem. 55, 204–210. https://doi.org/10.1007/BF02757200

Batchu, N.K., Binnemans, K., 2018. Effect of the diluent on the solvent extraction of neodymium(III) by bis(2-ethylhexyl)phosphoric acid (D2EHPA). Hydrometallurgy 177, 146–151. https://doi.org/10.1016/j.hydromet.2018.03.012

Binnemans, K., Jones, P.T., Blanpain, B., Van Gerven, T., Yang, Y., Walton, A., Buchert, M., 2013. Recycling of rare earths: a critical review. J. Clean. Prod. 51, 1–22. https://doi.org/10.1016/j.jclepro.2012.12.037

Chirachanchai, S., Phongtamrug, S., Tashiro, K., 2011. Supramolecular Chemistry of Benzoxazines, in: Handbook of Benzoxazine Resins. Elsevier, pp. 331–354. https://doi.org/10.1016/B978-0-444-53790-4.00062-X

Goward, G.R., Sebastiani, D., Schnell, I., Spiess, H.W., Kim, H.-D., Ishida, H., 2003. Benzoxazine Oligomers: Evidence for a Helical Structure from Solid-State NMR Spectroscopy and DFT-Based Dynamics and Chemical Shift Calculations. J. Am. Chem. Soc. 125, 5792–5800. https://doi.org/10.1021/ja029059r

Hogendoorn, C., Roszczenko-Jasińska, P., Martinez-Gomez, N.C., de Graaff, J., Grassl, P., Pol, A., Op den Camp, H.J.M., Daumann, L.J., 2018. Facile Arsenazo III-Based Assay for Monitoring Rare Earth Element Depletion from Cultivation Media for Methanotrophic and Methylotrophic Bacteria. Appl. Environ. Microbiol. 84, e02887-17. https://doi.org/10.1128/AEM.02887-17

Juère, E., Florek, J., Larivière, D., Kim, K., Kleitz, F., 2016. Support effects in rare earth element separation using diglycolamide-functionalized mesoporous silica. New J. Chem. 40, 4325–4334. https://doi.org/10.1039/C5NJ03147H

Kalam, S., Abu-Khamsin, S.A., Kamal, M.S., Patil, S., 2021. Surfactant Adsorption Isotherms: A Review. ACS Omega 6, 32342–32348. https://doi.org/10.1021/acsomega.1c04661

Kim, D., Powell, L., Delmau, L.H., Peterson, E.S., Herchenroeder, J., Bhave, R.R., 2016. A supported liquid membrane system for the selective recovery of rare earth elements from neodymium-based permanent magnets. Sep. Sci. Technol. 51, 1716–1726. https://doi.org/10.1080/01496395.2016.1171782

Laobuthee, A., Ishida, H., Chirachanchai, S., 2003. Metal Ion Guest Responsive Benzoxazine Dimers and Inclusion Phenomena of Cyclic Derivatives. J.

Incl. Phenom. Macrocycl. Chem. 47, 179–185. https://doi.org/10.1023/B:JIPH.0000011780.42898.09

Li, J., Zhu, X., Zhao, Y., Yang, M., Zhang, X., Chen, H., Liu, Q., 2025. Highly selective recovery of lanthanum and cerium from wastewater by amidoxime-modified biochar. Sep. Purif. Technol. 371, 133303. https://doi.org/10.1016/j.seppur.2025.133303

Li, L., Yu, B., Davis, K., King, A., Dal-Cin, M., Nicalek, A., Du, N., 2022. Separation of Neodymium (III) and Lanthanum (III) via a Flat Sheet-Supported Liquid Membrane with Different Extractant-Acid Systems. Membranes 12, 1197. https://doi.org/10.3390/membranes12121197

Martínez, J., Rodríguez Varela, R., Forsberg, K., Rasmuson, Å., 2018. Factors influencing separation selectivity of rare earth elements in flat sheet supported liquid membranes. Chem. Eng. Sci. 191, 134–155. https://doi.org/10.1016/j.ces.2018.06.018

Ni'am, A.C., Wang, Y.-F., Chen, S.-W., Chang, G.-M., You, S.-J., 2020. Simultaneous recovery of rare earth elements from waste permanent magnets (WPMs) leach liquor by solvent extraction and hollow fiber supported liquid membrane. Chem. Eng. Process. - Process Intensif. 148, 107831. https://doi.org/10.1016/j.cep.2020.107831

Petsagkourakis, I., Beni, V., Strandberg, J., Nilsson, M., Leandri, V., Lassen, B., Sandberg, M., 2024. Polymerisation of benzoxazine impregnated in porous carbons. A scalable and low-cost route to smart copper-ion absorbents with saturation indicator function. Process Saf. Environ. Prot. 184, 782–789. https://doi.org/10.1016/j.psep.2024.02.029

Taskin, O.S., Kiskan, B., Aksu, A., Balkis, N., Weber, J., Yagci, Y., 2014. Polybenzoxazine: A Powerful Tool for Removal of Mercury Salts from Water. Chem. – Eur. J. 20, 10953–10958. https://doi.org/10.1002/chem.201403200

Velazquez-Jimenez, L.H., Arcibar-Orozco, J.A., Rangel-Mendez, J.R., 2018. Overview of As(V) adsorption on Zr-functionalized activated carbon for aqueous streams remediation. J. Environ. Manage. 212, 121–130. https://doi.org/10.1016/j.jenvman.2018.01.072

Wannachod, T., Leepipatpiboon, N., Pancharoen, U., Phatanasri, S., 2015. Mass transfer and selective separation of neodymium ions via a hollow fiber supported liquid membrane using PC88A as extractant. J. Ind. Eng. Chem. 21, 535–541. https://doi.org/10.1016/j.jiec.2014.03.016

Wilfong, W.C., Kail, B.W., Wang, Q., Shi, F., Shipley, G., Tarka, T.J., Gray, M.L., 2020. Stable immobilised amine sorbents for heavy metal and REE removal from industrial wastewaters. Environ. Sci. Water Res. Technol. 6, 1286–1299. https://doi.org/10.1039/C9EW00915A

Yadoun, B., Benhamou, A., Hennous, M., Benyoub, N., Debab, A., 2024. Synthesis and application of SBA-15 adsorbent for the removal of organic and inorganic substances. Environ. Sci. Pollut. Res. 31, 57874–57886. https://doi.org/10.1007/s11356-024-34964-6

Zhang, F., Ma, K.-Q., Li, Y., Ran, Q., Yao, C.-Y., Yang, C.-T., Yu, H.-Z., Hu, S., Peng, S.-M., 2020. Selective separation of thorium from rare earths and uranium

in acidic solutions by phosphorodiamidate-functionalised silica. Chem. Eng. J. 392, 123717. https://doi.org/10.1016/j.cej.2019.123717

STOCKHOLM
Box 21060, 100 31 Stockholm

GOTHENBURG
Box 53021, 400 14 Gothenburg

MALMÖ
Nordenskiöldsgatan 24
211 19 Malmö

KRISTINEBERG
(Center for Marine Research and Innovation)
Kristineberg 566
451 78 Fiskebäckskil

SKELLEFTEÅ
Kanalgatan 59
931 32 Skellefteå

BEJING, CHINA
Room 612A
InterChina Commercial Building No.33
Dengshikou Dajie
Dongcheng District
Beijing 100006
China

This report has been reviewed and approved in accordance with IVL's audit and approval management system.